Evaluation of snow cover properties in ERA5 and ERA5-Land with several satellite-based datasets in the Northern Hemisphere in spring 1982-2018

Kerttu Kouki[1], Kari Luojus[1], Aku Riihelä[1]

[1]Finnish Meteorological Institute, Helsinki, P.O. Box 503, 00101, Finland

Correspondence to: Kerttu Kouki (kerttu.kouki@fmi.fi)

Abstract. Seasonal snow cover of the Northern Hemisphere (NH) greatly influences surface energy balance, hydrological cycle, and many human activities, such as tourism and agriculture. Monitoring snow cover at continental scale is only possible from satellites or using reanalysis data. The aim of this study is to analyze timeseries of surface albedo, snow water equivalent (SWE), and snow cover extent (SCE) in spring in ERA5 and ERA5-Land reanalysis data and to compare the timeseries with several satellite-based datasets. As satellite data for the SWE intercomparison, we use bias-corrected SnowCCI v1 data for non-mountainous regions and the mean of Brown, MERRA-2 and Crocus v7 datasets for the mountainous regions. For surface albedo, we use the black-sky albedo datasets CLARA-A2 SAL, based on AVHRR data, and MCD43D51 based on MODIS data. Additionally, we use Rutgers and JAXA JASMES SCE products. Our study covers land areas north of 40 °N and the period between 1982 and 2018 (spring season from March to May). The analysis shows that both ERA5 and ERA5-Land overestimate SWE. ERA5-Land shows larger overestimation, which is mostly due to very high SWE values over mountainous regions. The analysis revealed a discontinuity in ERA5 around year 2004, since adding IMS (Interactive Multisensor Snow and Ice Mapping System) from year 2004 onwards considerably improves SWE estimates but makes the trends less reliable. The negative NH SWE trends in ERA5 range from -249 Gt decade^{-1} to -236 Gt decade^{-1} in spring, which is two to three times larger than the trends detected by the other datasets (ranging from -124 Gt decade^{-1} to -77 Gt decade^{-1}). Albedo estimates are more consistent between the datasets with a slight overestimation in ERA5 and ERA5-Land. SCE is accurately described in ERA5-Land, whereas ERA5 shows notably larger SCE than the satellite-based datasets. The negative trends in albedo and SCE are strongest in May, when albedo trend varies from -0.011 decade^{-1} to -0.006 decade^{-1} depending on the dataset. The negative SCE trend detected by ERA5 in May (-1.22 million km^2 decade^{-1}) is about twice as large as the trends detected by other datasets (ranging from -0.66 million km^2 decade^{-1} to -0.50 million km^2 decade^{-1}). The analysis also shows that there is a large spatial variability in the trends, which is consistent with other studies.

1 Introduction

Seasonal snow cover of the Northern Hemisphere (NH) is an important part of the global climate system. In winter, a large fraction of incoming solar radiation is reflected back due to the high albedo of snow cover, whereas in summer, the darker

30 snow-free surface absorbs more incoming solar radiation (Callaghan et al., 2011; Flanner et al., 2011; Qu and Hall, 2005; Trenberth and Fasullo, 2009). Therefore, changes in snow cover will affect the surface albedo and, thus, the surface energy balance.

Albedo is the hemispherical reflectance of the surface, defined as the ratio between reflected and incoming solar radiative
35 fluxes (Ångström, 1925). The solar radiation that reaches the Earth's surface can be either direct or diffuse (Schaepman-Strub et al., 2006). When incoming solar radiation propagates through atmosphere, it can be scattered to different directions due to, for example, clouds and aerosols. A part of this scattered radiation reaches the surface, and it is called the diffuse solar radiation. The solar radiation that reaches the surface without being scattered, is called direct solar radiation. Albedo can be divided into different components based on the solar radiation: The surface albedo, including both direct and diffuse
40 solar radiation, is often referred as blue-sky albedo. The albedo for direct solar radiation is the directional-hemispherical reflectance, often also called black-sky albedo. The albedo for the diffuse radiation, in turn, is bi-hemispherical reflectance and called white-sky albedo (Schaepman-Strub et al., 2006). The blue-sky albedo is a weighted average of black-sky and white-sky albedos (Schaepman-Strub et al., 2006). Clouds affect the ratio between the diffuse and direct solar radiation and, therefore, the changes in cloudiness also affect the blue-sky albedo (Key et al., 2001). Typically, the values for white-sky
45 albedo are larger than the values for black-sky albedo, and blue-sky albedo is somewhere between these two (Manninen et al., 2012; Manninen et al., 2019; Schaepman-Strub et al., 2006).

Snow cover affects many human activities, such as road traffic, tourism, forestry, and agriculture (Callaghan et al., 2011). In the high latitudes and in the mountainous regions, snow cover also greatly influences the hydrological cycle (Barnett et al.,
50 2005; Bormann et al., 2018; Callaghan et al., 2011; Douville et al., 2002; Li et al., 2017). In winter, snow cover stores a large amount of fresh water and limits water availability. When snow melts in spring and summer, water is released and redistributed. Melting snow is an important source of fresh water, as about one-sixth of the world's population depends on melt water from snow (Barnett et al., 2005). Hydropower production is also dependent on meltwater from snow (Callaghan et al., 2011; Magnusson et al., 2020). In many regions, most of the annual inflow to hydropower reservoirs often comes
55 during the spring snowmelt period (Magnusson et al., 2020). Therefore, changes in snow cover can cause both water shortages and affect hydropower production.

The global air temperature is rising due to climate change which causes the melt season to begin earlier and affects the timing of the streamflow peaks (Kundzewicz et al., 2008; Musselman et al., 2021). Rising temperatures also cause the winter
60 precipitation to shift from snow to rain, which affects the intensity of the streamflow during melt season (Kundzewicz et al., 2008). The streamflow is projected to decrease especially in USA and southern and central Europe (van Vliet et al., 2016). For example, in USA, snow is the largest source of water storage in the arid western states (Hall et al., 2008; Li et al., 2017), where the Colorado River, which originates from the Rocky Mountains, highly depends on the melt water from snow (Li et

al., 2017). The river provides drinking water to 40 million people and irrigates over five million acres of agricultural land

65 across seven states in the USA and two in Mexico (Smith et al., 2022). The warming climate will cause snowpack losses in the Rocky Mountains, which will, in turn, affect the availability of water in Colorado River basin states (Hall et al., 2008; Kundzewicz et al., 2008, Li et al., 2017).

Studies have shown that seasonal snow cover is changing, and snow cover in spring is especially sensitive to warming

70 (Derksen and Brown, 2012). In winter, there is not much sunlight in the Arctic, so changes in snow cover have a smaller effect on the surface energy budget. In spring, the amount of incoming solar radiation increases, which also makes the surface albedo feedback (SAF) stronger. Since there is still a lot of snow in the Arctic in the spring season, changes in the spring snow cover greatly affect the surface energy balance and, thus, the climate system (Déry and Brown, 2007).

75 Snow water equivalent (SWE) is the amount of water that would result, if the snowpack would melt instantaneously, and it can be expressed in the units of mm or, equivalently, in the units of kg m^{-2} (Fierz et al., 2009). Recent studies show negative trends in global SWE and in the extent and duration of NH snow cover, but seasonal and spatial variability exists (Bormann et al., 2018; Derksen and Mudryk, 2022; Hernández-Henríquez et al., 2015; Pulliainen et al., 2020). In early winter from October to December, most datasets show negative trends in snow cover extent (SCE), while in January and February, there

80 are no significant trends (Mudryk et al., 2017). The observed snow cover trends in spring are clearly negative in both Eurasia and North America (Derksen and Brown, 2012; Essery et al., 2020; Hernández-Henríquez et al., 2015). Also, a clear trend exists towards earlier melt season (Metsämäki et al., 2018; Takala et al., 2009; Tedesco et al., 2009). SWE shows large spatial variability; in North America, there is a negative trend in observed SWE, whereas in Eurasia the trends are less prominent. In Siberia, there are also regions where SWE is observed and projected to increase (Pulliainen et al., 2020;

85 Räisänen, 2008).

Particularly in the Arctic regions, snow cover plays a significant role in the climate system, making it crucial to understand the characteristics of the snow cover in these areas. As in situ measurement network is relatively sparse, snow cover monitoring at continental scale is only possible from satellites or using reanalysis data. Both methods can cover large areas

90 and provide snow cover estimates also in those regions which lack in situ observations and are therefore widely used in climate research (e.g., Mortimer et al., 2020; Mudryk et al., 2020).

Reanalyses provide decadal time series with multiple variables making them suitable for various kind of research, and they have become an important part of climate studies. ERA5 is the fifth generation ECMWF (European Centre for Medium-

95 Range Weather Forecasts) atmospheric reanalysis replacing the older ERA-Interim reanalysis (Hersbach et al., 2020). ERA5 uses advanced modeling and data assimilation systems and combines large amounts of historical observations into global estimates. ERA5-Land, in turn, is the land component from ERA5 with a finer spatial resolution (Muñoz-Sabater et al.,

3

2021). It is produced without coupling the atmospheric module, and it runs without data assimilation making it computationally lighter (Muñoz-Sabater et al., 2021).

100

Snow cover properties in ERA5 and ERA5-Land have been evaluated in several studies (e.g., Mortimer et al., 2020; Urraca and Gobron, 2021; Räisänen, 2023). Overall, ERA5 and ERA5-Land have been found to perform well compared to other reanalyses (Jia et al., 2022; Lei et al., 2022; Mortimer et al., 2020). However, studies have shown that ERA5 tends to overestimate snow cover extent, SWE, and surface albedo (Bian et al., 2019; Guo and Yang, 2022; Orsolini et al., 2019;

105 Xiaona et al., 2020). Also, ERA5-Land shows a slight overestimation in surface albedo during snow-free season (Jia et al., 2022). ERA5 slightly underestimates very deep snow especially late in the snow season and shows delayed ablation of deep snowpack in spring (Lei et al., 2022; Mortimer et al., 2020). ERA5-Land SWE estimates agree well with other reanalysis datasets but struggles in comparison with satellite-based data (Räisänen, 2023). ERA5-Land shows especially large overestimation over mountainous areas (Monteiro and Morin, 2023). Also, a discontinuity in 2004 has been observed in

110 ERA5 snow cover estimates, which is due to adding IMS information in ERA5 (Urraca and Gobron, 2021; Mortimer et al., 2020). This discontinuity has improved the accuracy of snow cover estimates after year 2004 considerably, but decreased the temporal stability (Urraca and Gobron, 2021).

Even though several studies exist on evaluating either ERA5 or ERA5-Land, few studies exist on comparing snow cover

115 properties in ERA5 and ERA5-Land. Lei et al. (2022) studied the effect of spatial resolution on snow depth estimates over the Tibetan Plateau and found that the finer-resolution ERA5-Land is more consistent with in situ measurements than ERA5. Li et al. (2022) found that both ERA5 and ERA5-Land tend to overestimate snow depth at high elevation in Central Asia. Monteiro and Morin (2023) have assessed the performance of several reanalyses, including ERA5 and ERA5-Land, over the European Alps and concluded that ERA5-Land considerably overestimates SWE, while ERA5 is better in line with the

120 reference data. Urraca and Gobron, (2021) studied snow cover duration and the stability of the trends in ERA5 and ERA5-Land over NH but did not consider other variables related to snow cover. Thus, our study is to the authors' knowledge the first, where NH snow cover properties (SWE, SCE, and albedo) are compared between ERA5 and ERA5-Land and evaluated with several satellite-based datasets.

2 Data and Methods

125 ### 2.1 ERA5 and ERA5-Land

The datasets used in this study are listed in Table 1. ERA5 is the fifth generation ECMWF atmospheric reanalysis replacing the older ERA-Interim (Hersbach et al., 2020). ERA5 covers years from 1950 onwards with a grid resolution of 31 km, which is a considerably higher spatial resolution than in ERA-Interim (80 km). ERA5 is based on Integrated Forecasting System (IFS) Cycle 41r2 and it provides hourly fields for all variables. Additionally, it provides pre-computed monthly

130 means (Hersbach et al., 2020), which we used in this study. The number of observations assimilated in ERA5 increases constantly throughout the production period. ERA5 assimilates snow depth information from several SYNOP stations, and from year 2004 onwards, it also uses IMS data over NH (Hersbach et al., 2020).

ERA5-Land, in turn, is a replay of the land component of ERA5 with a finer spatial resolution (9 km) (Muñoz-Sabater et al.,
135 2021). It is produced with land model H_TESSEL and without coupling the atmospheric module. Also, ERA5-Land runs without data assimilation, which makes it computationally lighter (Muñoz-Sabater et al., 2021).

Our study includes three variables: SWE, SCE, and albedo. SWE was directly available in both ERA5 and ERA5-Land (variable "sd"). In ERA5-Land, snow cover fraction in a grid cell (SC) is directly available (variable "snowc"), but for
140 ERA5, we calculated SC in a grid cell using snow density and SWE:

$$SC = \frac{\rho_w \cdot SWE\ [m]}{\rho_{snow}} \cdot \frac{1}{0.1} \qquad\qquad (1)$$

where ρ_w is the density of water (1000 kg m^{-3}) and ρ_{snow} is the density of snow. We calculated SCE by multiplying snow
145 cover fraction in a grid cell (SC) with the size of the grid cell.

ERA5 and ERA5-Land provide several estimates for albedo. Both ERA5 and ERA5-Land have directly available the albedo for diffuse radiation, i.e., the white-sky albedo (variable "fal"). Also, ERA5 and ERA5-Land provide radiation estimates from which blue-sky albedo can be computed. Additionally, ERA5 has radiation estimates for clear-sky conditions from
150 which blue-sky albedo for clear-sky can be calculated. Thus, we calculated the blue-sky albedo (α_{blue}) using downward solar radiation (SW$_{dn}$; variable "ssrd") and net solar radiation (SW$_{net}$; variable "ssr"):

$$\alpha_{blue} = 1 - \frac{SW_{net}}{SW_{dn}} \qquad\qquad (2)$$

155 Similarly, blue-sky albedo for clear-sky (α_{clear}) was calculated using Eq. (2) with the radiation estimates for clear skies (downward solar radiation for clear skies, variable "ssrdc", and net solar radiation for clear skies, variable "ssrc").

We compared the timeseries of all these albedo estimates (Fig. S1) and the analysis showed that the different albedo estimates are very close to each other in both ERA5 and ERA5-Land. The satellite-based products (Sect 2.2) provide
160 estimates for black-sky albedo, which is not available in ERA5 or ERA5-Land. From the variables shown in Fig. S1, the blue-sky albedo for clear-sky (α_{clear}) would typically be closest estimate to black-sky albedo, whereas white-sky albedo is typically the furthest away from black-sky albedo. However, the blue-sky albedo for clear-sky (α_{clear}) is only available in

ERA5 and not in ERA5-Land. Therefore, we decided to use the blue-sky albedo (α_{blue}) in this analysis, as it is available in both ERA5 and ERA5-Land. This issue is further discussed in Sect 2.2.

165

Table 1. Datasets used in this study.

Variable	Dataset	Resolution	Reference
SWE SW_{dn} SW_{net} $SW_{dn,clear}$ $SW_{net,clear}$ ρ_{snow}	ERA5	31 km × 31 km, monthly	Hersbach et al. (2020)
SWE SCE SW_{dn} SW_{net}	ERA5-Land	9 km × 9 km, monthly	Muñoz-Sabater et al. (2021)
SWE	Bias-corrected SnowCCI v1	25 km × 25 km, monthly	Luojus et al. (2021)
SWE	Brown	0.75° × 0.75°, monthly	Brown et al. (2003)
SWE	Crocus v7	0.5° × 0.5°, monthly	Brun et al. (2013)
SWE	MERRA-2	0.5° × 0.625°, monthly	Gelaro et al. (2017) GMAO (2015)
SCE	Rutgers	24 km × 24 km, weekly	Robinson and Estilow (2021)
SCE	JAXA JASMES	5 km × 5 km, half-monthly	Hori et al. (2017)
Black-sky albedo	CLARA-A2 SAL	0.25° × 0.25°, monthly	Anttila et al. (2016) Karlsson et al. (2017)
Black-sky albedo	MCD43D51	30 arcsec × 30 arcsec, daily	Schaaf and Wang (2021a)
Quality information	MCD43D31	30 arcsec × 30 arcsec, daily	Schaaf and Wang (2021b)

2.2 Satellite-based datasets

The SWE reference data used in this study consists of four datasets: ESA CCI Snow "SnowCCI" (European Space Agency

170   Climate Change Initiative, Snow) v1 data (Luojus et al., 2021), MERRA-2 (the Modern-Era Retrospective analysis for Research and Applications, Version 2; Gelaro et al., 2017; GMAO, 2015a), Brown (Brown et al., 2003), and Crocus v7 (Brun et al., 2013).

SnowCCI v1 is the same product as the GlobSnow v3 SWE product except provided in geographical latitude-longitude grid

175   for easier comparison with climate model data. The product is based on satellite-based microwave brightness temperature data and ground-based snow depth measurements (Luojus et al., 2021). Subsequently, the dataset is bias-corrected with extensive ground-based snow course measurements, which decrease the uncertainty of hemisphere-mean SWE estimates notably (Pulliainen et al., 2020). We have used SnowCCI v1, even though there is already version 2 available. Version 2 (v2) has been shown to underestimate SWE and currently, the bias-corrected SnowCCI v1 is considered to be the best SWE

180   estimate when analyzing decadal timeseries (Mortimer et al., 2022). A notable difference between v1 and v2 is that v1 uses constant snow density, while v2 uses spatially and temporally varying snow densities (Mortimer et al., 2022). The dynamic snow density decreases the annual maximum SWE, which leads to underestimation of SWE in v2. Therefore, v1 currently provides more reliable SWE estimates, and the bias-corrections further improve v1 making the bias-corrected SnowCCI v1 currently the best SWE estimate (Mortimer et al., 2022). The SnowCCI data are available for the period 1979-2018 and are

185   mapped to a 25 km EASE-Grid (Luojus et al., 2021).

As the SnowCCI data are only available for non-mountainous regions, we have used the mean of the MERRA-2, Brown, and Crocus v7 SWE products for the mountainous regions. MERRA-2 is a NASA (National Aeronautics and Space Administration) atmospheric reanalysis, and it is available from year 1980 (Gelaro et al., 2017). Brown SWE product, in

190   turn, uses a simple snow scheme driven by ERA-Interim reanalysis (Brown et al., 2003). Crocus version 7 product is a physical snow model driven by ERA-Interim reanalysis (Brun et al., 2013). Both MERRA-2 and Crocus v7 tend to slightly overestimate SWE under 150 mm and underestimate SWE over 150 mm (Mortimer et al., 2020).

We used two satellite-based surface albedo products in this study. CLARA-A2 SAL (Clouds, Albedo and Radiation second

195   release Surface Albedo) product provides the broadband shortwave directional-hemispherical reflectance, i.e., the black-sky albedo (Anttila et al., 2016a; Karlsson et al., 2017). The product is based on AVHRR (Advanced Very High Resolution Radiometer) data, and the data are available for the period 1982-2019. We used the monthly mean values with spatial resolution of $0.25° \times 0.25°$ on a regular latitude-longitude grid. The mean relative retrieval error is -0.6%, the mean root mean square error is 0.075 and the decadal relative stability (over Greenland Summit) is 8.5% (Anttila et al., 2016b). The

200   product has been found to perform especially well over snow and ice, which makes it well-suited for cryospheric studies over the Arctic (Anttila et al., 2016b).

Additionally, we used the MCD43D51 product which is the black-sky albedo for the MODIS shortwave broadband (Schaaf and Wang, 2021a). It is a daily product with a grid resolution of 30 arc second (1 km) and available from year 2000 onwards.

205   We also used the quality information (MCD43D31) for the albedo product (Schaaf and Wang, 2021b) and only included pixels with good quality in the analysis, which ensures the high accuracy of the product.

The satellite-based albedo products provide black-sky albedo estimates, whereas ERA5 and ERA5-Land albedo estimates are for blue sky-albedo, which can cause a slight uncertainty in the comparison. ERA5 would also provide blue-sky albedo

210 for clear-sky, which would typically be closer to black-sky albedo. However, that is not available in ERA5-Land, so we decided to use the blue-sky albedo to maintain consistency between ERA5 and ERA5-Land. Also, the comparison of the different albedo estimates in ERA5 and ERA5-Land showed that the differences between the different albedo estimates is negligible (Fig. S1). Studies have also shown that the difference between black-sky and blue-sky is less than 5 % with low aerosol optical depth (AOD) values (Manninen et al., 2012), which is typical for the Arctic region (Shikwambana and

215 Sivakumar, 2018). Therefore, we decided not to make any adjustments to any of the albedo datasets in order to minimize the possible discrepancies between black-sky and blue-sky albedo estimates. This approach has been used also in previous studies (e.g., Riihelä et al., 2013; Pohl et al., 2020). For simplicity, from now on, we will simply refer to albedo and do not differentiate between different types of albedos unless the difference is relevant.

220 The SCE products used in this study are the Rutgers weekly product (Robinson and Estilow, 2021) and JAXA JASMES SCE product (Hori et al., 2017). The Rutgers product provides weekly SCE at 24 km resolution. It is a binary product (no snow or snow-covered), and the threshold for which a grid cell is considered snow covered is 50% or greater (Robinson and Estilow, 2021). The data are available from year 1980 onwards. The Rutgers weekly SCE product at 190 km resolution has been widely used in climate research (e.g., Brown et al., 2010; Déry and Brown, 2007; Hernández-Henríquez et al., 2015), as the

225 dataset is available from year 1966 onwards making it the longest running satellite-based SCE record (Estilow et al., 2015). Recently, the product was gridded to a finer resolution, as the weekly SCE maps spanning from 1980 through 1999 were digitized at 24 km resolution. Since 1999, the SCE charts have been produced daily at 24 km resolution using the IMS data (Robinson and Estilow, 2021). Especially before IMS period, the data are most accurate with cloud-free conditions, stable or slow-changing snow cover and high solar illumination levels (Robinson and Estilow, 2021).

230

The JAXA JASMES product is based on AVHRR and MODIS data (Hori et al., 2017). The product provides the snow cover fraction (0-100%) at 5 km resolution and is available from year 1978 onwards. The product uses AVHRR before 2000 and MODIS data from year 2000 onwards (Hori et al., 2017). Studies have shown that JAXA JASMES tends to slightly overestimate SCE and the overestimation increases in spring. However, the overall accuracy of the dataset is very high (Hori

235 et al., 2017). Rutgers shows higher SCE than JAXA JASMES in the Arctic (north of 60°N) in May (Derksen and Mudryk, 2022).

2.3 Methods

We have used the nearest neighbor method to resample ERA5, ERA5-Land, Brown, Crocus, MERRA-2, Rutgers and JAXA JASMES to 25 km equal-area projection. The higher-resolution MODIS albedo product was first coarsened to 0.25°

240   resolution by calculating the mean value of all the grid cells within one 0.25° × 0.25° grid cell and subsequently resampled to 25 km equal-area projection using the nearest neighbor method. We have used monthly mean values for each variable. The snow cover extent (SCE) was calculated by multiplying the area of one grid cell (25 km × 25 km) with the snow cover fraction in each grid cell. Our study covers land areas north of 40° N (glaciers and ice sheets are excluded) and the period between 1982-2018 (spring season from March to May). As MODIS data are available only from year 2000 onwards, we

245   have done some analysis additionally for the period 2000-2018.

To study the trends, we used the Theil-Sen estimator (Sen, 1968; Theil, 1950), which is the median of all slopes between paired values, and it is less sensitive to outliers than the ordinary least squares linear regression. We calculated trends for the entire study area (Sect. 3.1) and separately for Eurasia and North America (Sect. 3.2). Additionally, we computed the trends

250   in each grid cell (Sect. 3.3) to study the spatial variability of the trends. If there were missing values when calculating the trends in each grid cell, we calculated trends only in grid cells with at least 15 values available during the study period (i.e., at least 15 years of data).

3 Results

Figure 1 shows as an example the mean values for each of the dataset in April 1982-2018 (MODIS 2000-2018). Overall, the

255   spatial distributions of SWE, albedo and SCE are quite similar in ERA5, ERA5-Land and the satellite-based datasets. SWE shows large spatial variability in all the datasets. The highest monthly mean values exceed 240 mm, and these are found in Rocky Mountains, southeastern Canada, Scandinavia and in Siberia. However, in ERA5 and ERA5-Land, the areas with very high SWE values are more extensive than in the SWE reference data, indicating that both ERA5 and ERA5-Land overestimate SWE compared to the SWE reference data. Also, ERA5-Land seems to overestimate SWE even more than

260   ERA5.

Albedo shows highest values in the northern part of the study area, and the spatial distribution is similar to the SWE distribution. All the albedo datasets are quite consistent with each other. When comparing ERA5 and ERA5-Land, ERA5-Land shows slightly higher values than ERA5. Spatial distribution of SCE is consistent between ERA5-Land, Rutgers and

265   JAXA JASMES, whereas ERA5 shows clearly larger SCE.

3.1 Timeseries and trends in NH

Both ERA5 and ERA5-Land notably overestimate SWE sum over the entire study area in every month in spring compared to the SWE reference data (Fig. 2, top row). ERA5-Land shows even higher values than ERA5, which was evident also in Fig. 1. The magnitude of the difference stays about the same (Fig. 2, second row) throughout the spring season indicating

270   that in late spring the relative difference is very large. The values in ERA5 and ERA5-Land are about two times higher in

March and almost three times higher in May compared to the SWE reference data. The difference between ERA5-Land and SWE reference data stays around 3000 Gt throughout the study period. For ERA5, in turn, there is a clear drop in the difference around year 2004, which is the year when IMS data was added to the reanalysis. The drop is more visible in March and April than in May.
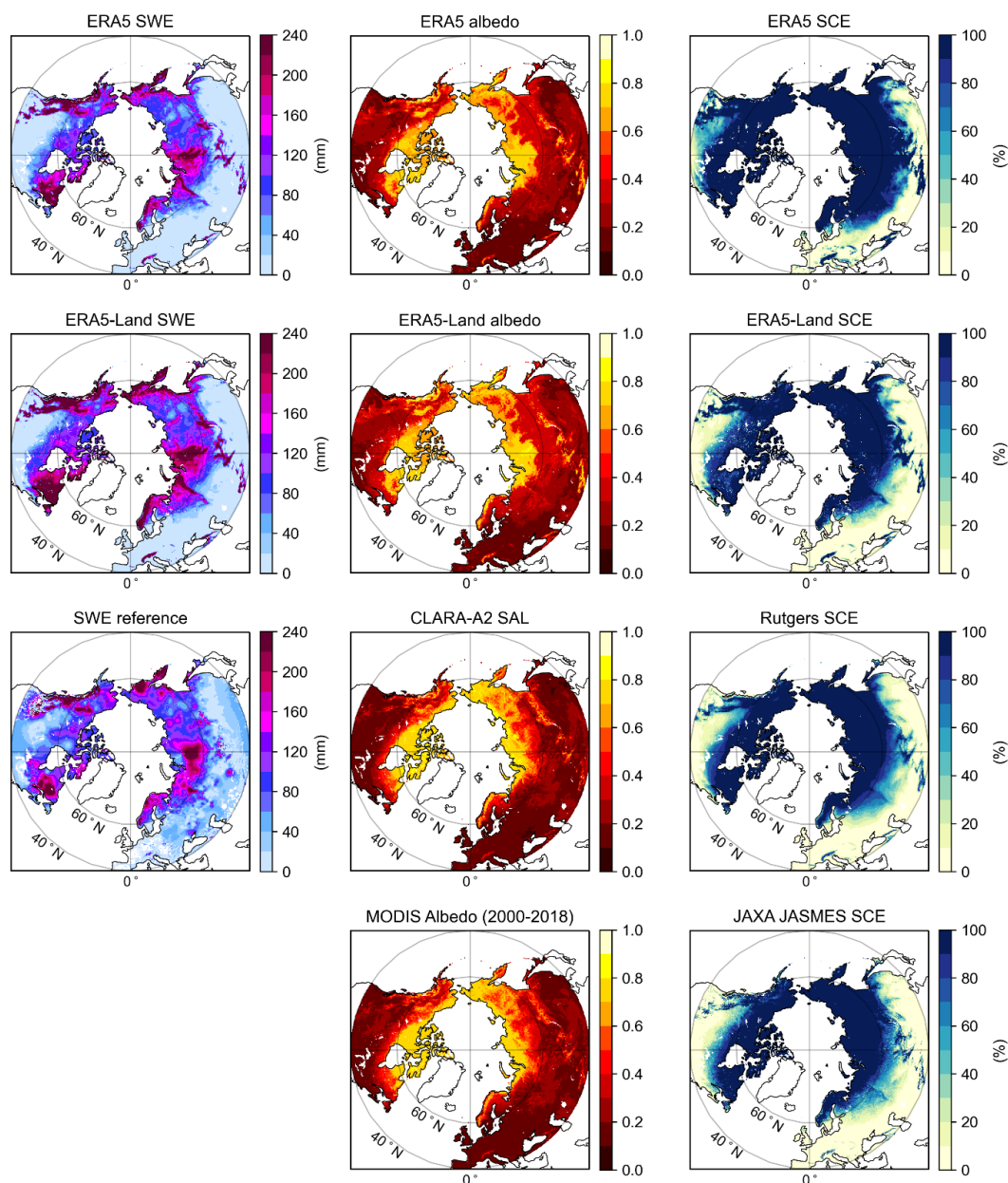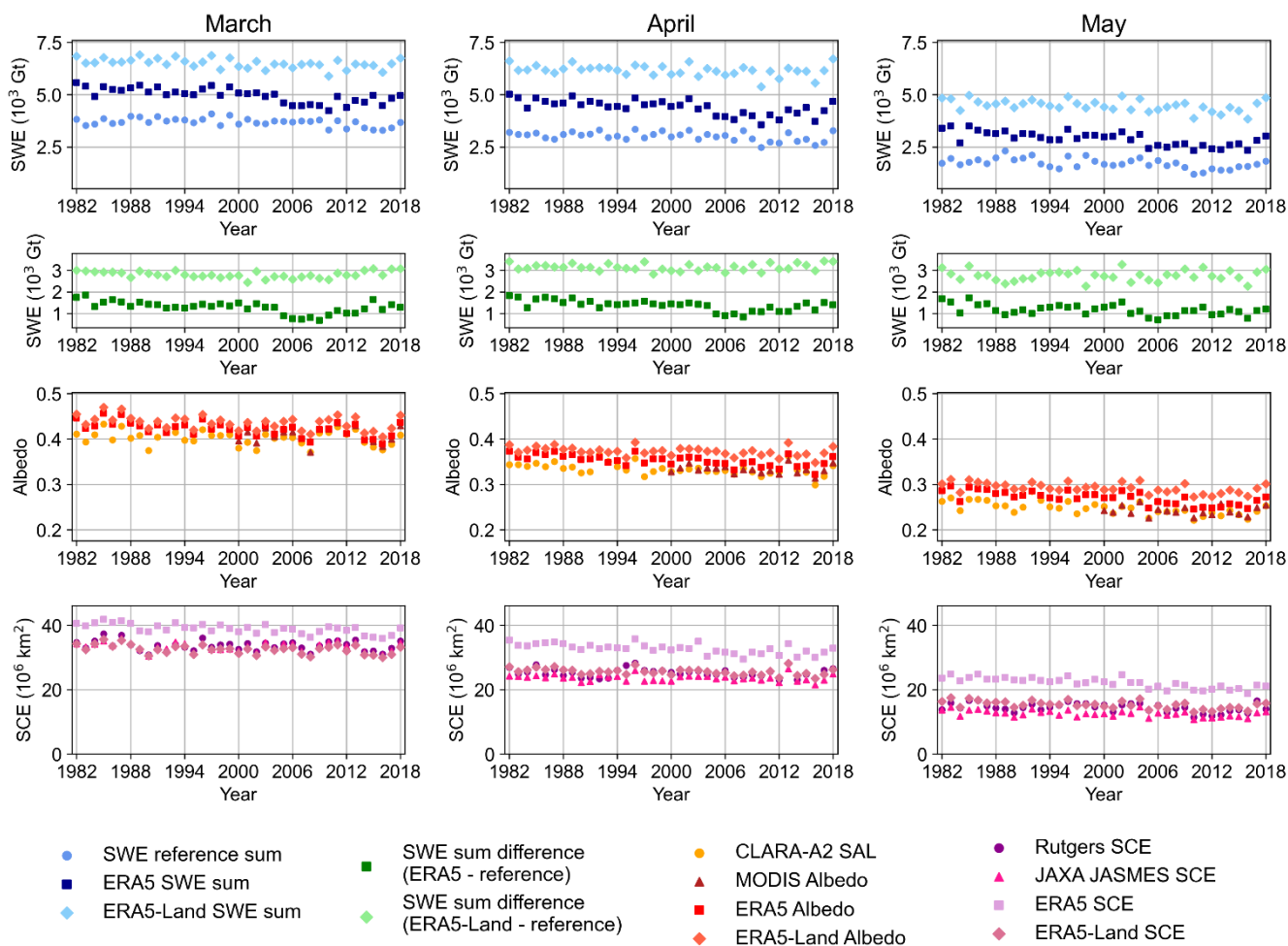

Figure 1. Mean values in April 1982-2018 for each of the datasets (MODIS 2000-2018).

Figure 2. Timeseries in the whole study area in (left) March, (middle) April and (right) May for SWE sum (top row), difference in SWE sum (second row), albedo (third row) and SCE (bottom row).

The timeseries for non-mountainous regions are shown in the Supplementary material (Fig. S2). The SWE values between the datasets are more consistent with each other, indicating that most of the overestimation in SWE occurs in the mountainous regions. Especially ERA5 is very well in line with the satellite-based dataset after year 2004.

The albedo timeseries (Fig. 2, third row) are more consistent with each other, which was already seen in Fig. 1. There is a slight overestimation in albedo in both ERA5 and ERA5-Land compared to CLARA-A2 SAL and MODIS data, but the

overestimation is not as prominent as in SWE. Even though ERA5 and ERA5-Land slightly overestimate albedo, both are
290 able to capture the annual variability quite well.

The SCE timeseries (Fig. 2 bottom row) show similar values for ERA5-Land, Rutgers and JAXA JASMES. ERA5, in turn,
show considerably larger SCE, which is consistent with Fig. 1. There is a slight drop in ERA5 SCE estimates in year 2004,
but it is not visible in albedo timeseries. Also, the timeseries of albedo and SCE for the non-mountainous regions (Fig. S2)
295 do not differ much from Fig 2., which is most likely due to the fact that even though mountain areas store a considerable
portion of snow mass (Kim et al., 2021), they only represent a small fraction of the whole study area. Therefore, they have
limited effect on SCE and albedo.
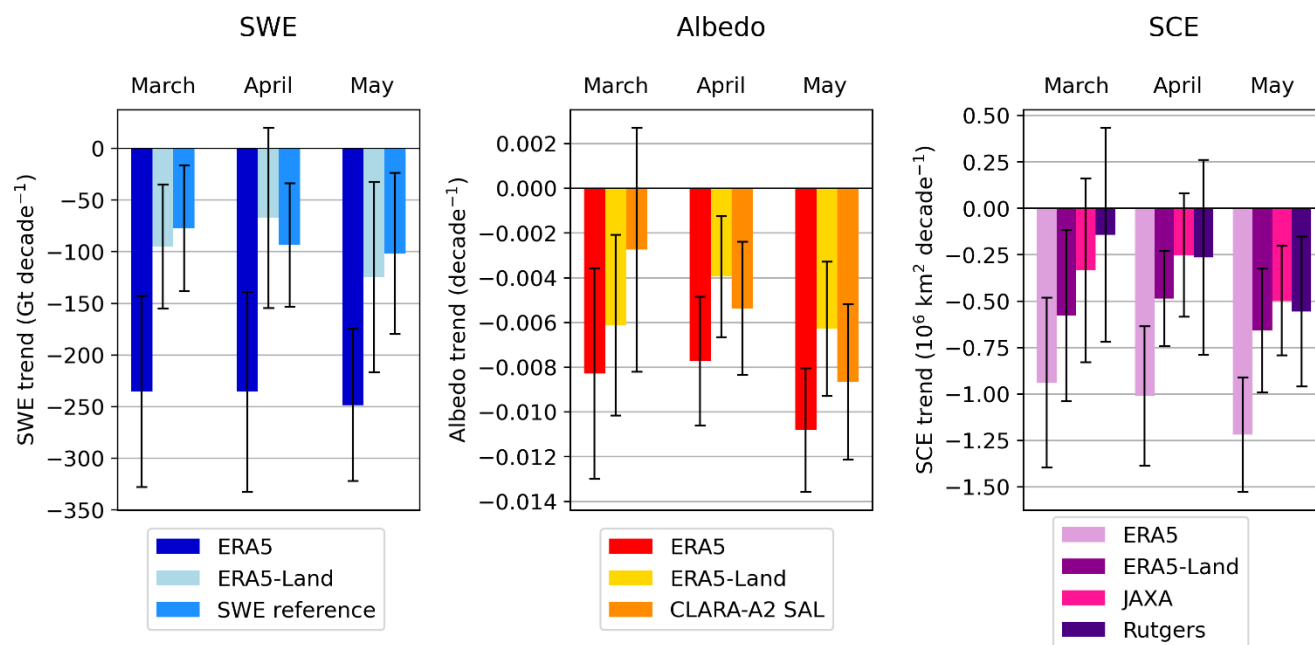
Figure 3. Trends in Northern Hemisphere in 1982-2018. The error bars represent the 95% confidence intervals.

Figure 3 summarizes the decadal trends and the 95% confidence intervals of the trends for each of the dataset. ERA5 shows
clearly negative SWE trends in every month (ranging from -249 Gt decade[-1] to -236 Gt decade[-1]). The trends in ERA5-Land
305 and the SWE reference data are also negative but not as prominent (ranging from -124 Gt decade[-1] to -77 Gt decade[-1]), which
means that ERA5 shows two or even three times larger decreasing trend than ERA5-Land and the SWE reference data.
Overall, the trends in ERA5-Land and SWE reference data are more consistent with each other, compared to ERA5. In
March, the difference between the trends in ERA5 and SWE reference cannot be explained with the uncertainties. All

datasets show statistically significant negative trends in March and May. In April, ERA5 and SWE reference data show
310   statistically significant negative trends.

The trends in albedo are more consistent between all the datasets. In March, CLARA-A2 SAL indicates that there is no
statistically significant trend, contrary to ERA5 and ERA5-Land. In April and May, all three datasets show statistically
significant trends, and the negative trends are strongest in May, when they vary from -0.011 decade^{-1} to -0.006 decade^{-1}.
315   Consistent with SWE, ERA5 shows more prominent trends in each month than ERA5-Land and CLARA-A2 SAL.

The trends in SCE show large variability between the datasets. In March and April, both ERA5 and ERA5-Land show
statistically significant negative trends, whereas the satellite-based JAXA JASMES and Rutgers indicate that there is not a
statistically significant trend. In May, all the datasets show statistically significant negative trends, but the negative trend
320   detected by ERA5 (-1.22 million km^2 decade^{-1}) is about twice as large as the trends detected by other datasets (ranging from
-0.66 million km^2 decade^{-1} to -0.50 million km^2 decade^{-1}). Climate warming affects the snow cover in late spring and
summer the most, while the changes in snow cover in late winter and early spring are minor (Derksen and Brown, 2012;
Mudryk et al., 2017). This also affects the uncertainties, as the wide uncertainty range in March clearly decreases towards
April and May. Similar to SWE and albedo, ERA5 shows the most prominent SCE trends in each month.

325   **3.2 Timeseries and trends in North America and Eurasia**

Figures 4 and 5 show the timeseries of SWE sum, albedo and SCE in North America and Eurasia. In North America, ERA5
and ERA5-Land show considerably larger values than the SWE reference data (Fig. 4, top row). The magnitude of the SWE
difference stays about the same throughout the spring season, which is consistent with Fig. 2. A drop in the difference
between ERA5 and the SWE reference data can be observed also in North America. In Eurasia (Fig. 5, top row), ERA5-Land
330   overestimates SWE considerably, whereas ERA5 is better in line with the SWE reference data. There is a clear difference
between ERA5 and SWE reference data in the beginning of the study period, but the difference decreases throughout the
study period, and after year 2004, the difference drops close to zero.

The albedo and SCE timeseries in North America and Eurasia (Figs. 4 and 5) show similar features than the timeseries in the
335   entire study area (Fig. 2). ERA5 and ERA5-Land show a slight overestimation in albedo and ERA5 overestimates SCE in
both North America and Eurasia.

Figures 6 and 7 summarize the decadal trends and the 95% confidence intervals in North America and Eurasia. In North
America (Fig. 6), ERA5 shows statistically significant negative trends in SWE in every month (ranging from -70 Gt decade^{-1}
340   to -57 Gt decade^{-1}), whereas ERA5-Land indicates that there is no trend at all. The SWE reference data, in turn, shows
negative trends in March (-77 Gt decade^{-1}) and May (-41 Gt decade^{-1}). All the albedo datasets indicate that there is no trend

in March or April, whereas in May, all the datasets show statistically significant negative trend (ranging from -0.009 decade^{-1} to -0.006 decade^{-1}). SCE also shows no trends, except ERA5 in March (-0.14 million km^2 decade^{-1}) and May (-0.26 million km^2 decade^{-1}).
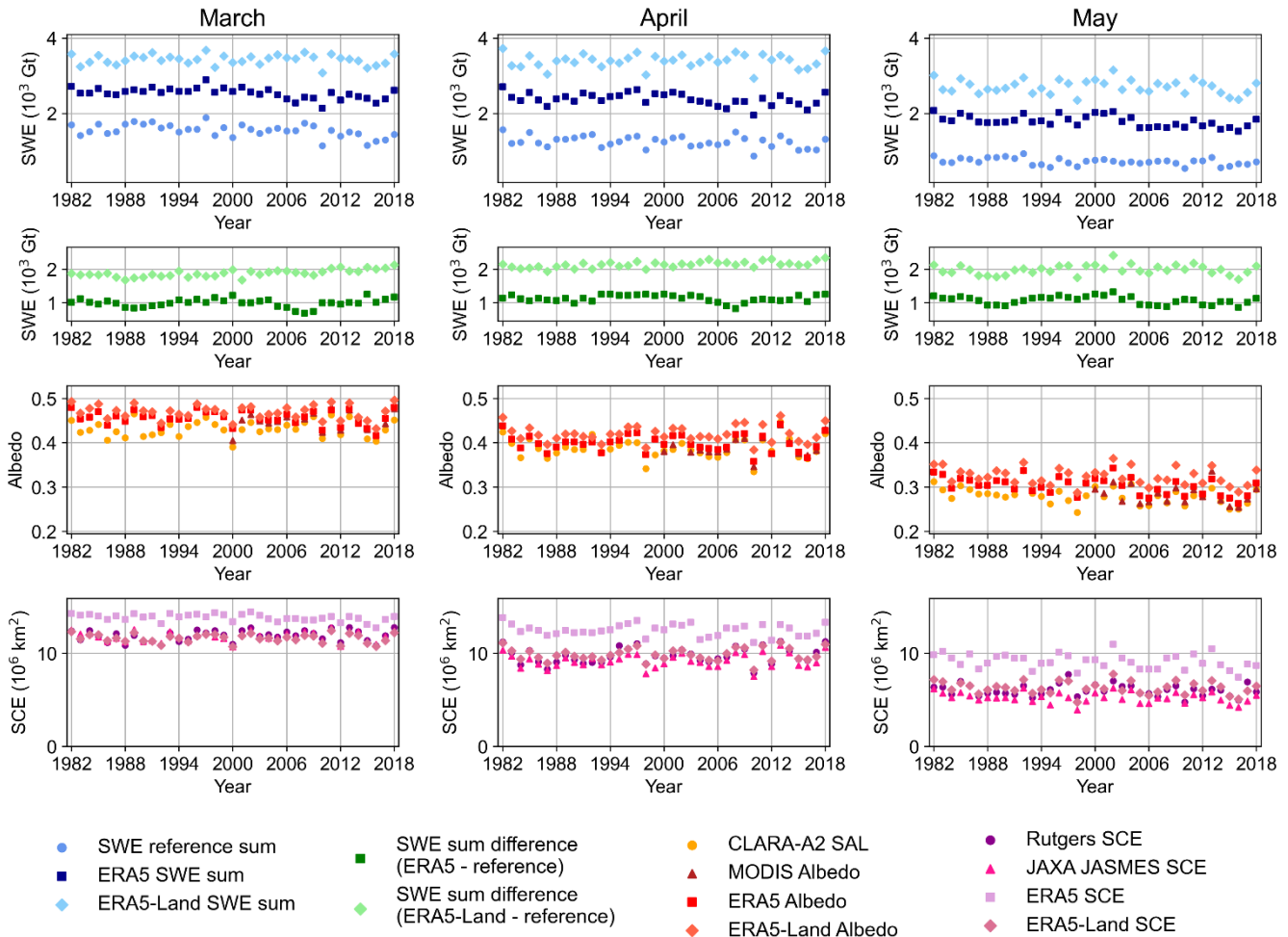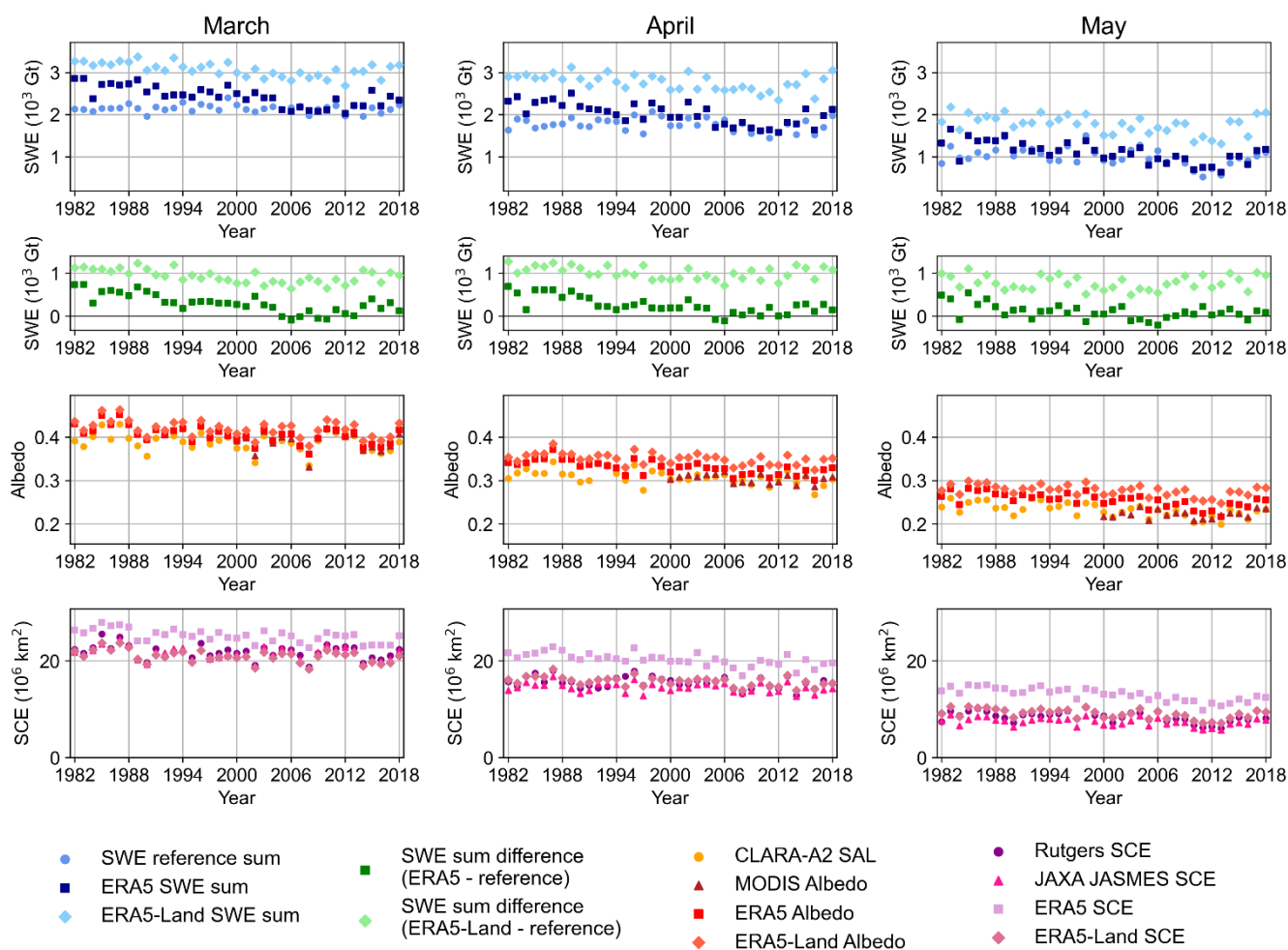
345

Figure 4. Timeseries in North America in (left) March, (middle) April and (right) May for SWE sum (top row), difference in SWE sum (second row), albedo (third row) and SCE (bottom row).

350 In Eurasia (Fig. 7), both ERA5 and ERA5-Land indicate a statistically significant negative trend in every month, whereas the SWE reference data detect no trend at all, which is consistent with previous studies (Pulliainen et al., 2020). For ERA5, the SWE trend ranges from -191 Gt decade^{-1} to -180 Gt decade^{-1} and for ERA5-Land from -105 Gt decade^{-1} to -102 Gt decade^{-1}. Especially in March, the trend is very close to zero according to the SWE reference data and becomes more prominent towards May, when the trend is -65 Gt decade^{-1}. There is a considerable difference in trends between ERA5, ERA5-Land

14

355   and the SWE reference data, which cannot be explained even with the uncertainties. The trends in albedo and SCE look similar to the ones detected in the whole study area (Fig. 3). In March, CLARA-A2 SAL indicates that there is not a statistically significant trend, but in April and May, all three datasets show statistically significant negative trends (ranging from -0.005 decade^{-1} to 0.011 decade^{-1}). ERA5 and ERA5-Land show statistically significant SCE trends in every month, whereas JAXA JASMES and Rutgers only detect negative trends in May. The negative SCE trends detected by ERA5

360   (ranging from -0.78 million km^2 decade^{-1} to -0.99 million km^2 decade^{-1}) are about twice as large as the trends detected by other datasets (ranging from -0.53 million km^2 decade^{-1} to -0.31 million km^2 decade^{-1}). Trends in both albedo and SCE intensify as spring progresses, which was also evident in the whole study area (Fig. 3). Overall, the trends are more prominent in Eurasia than in North America.

365   **Figure 5. Timeseries in Eurasia in (left) March, (middle) April and (right) May for SWE sum (top row), difference in SWE sum (second row), albedo (third row) and SCE (bottom row).**
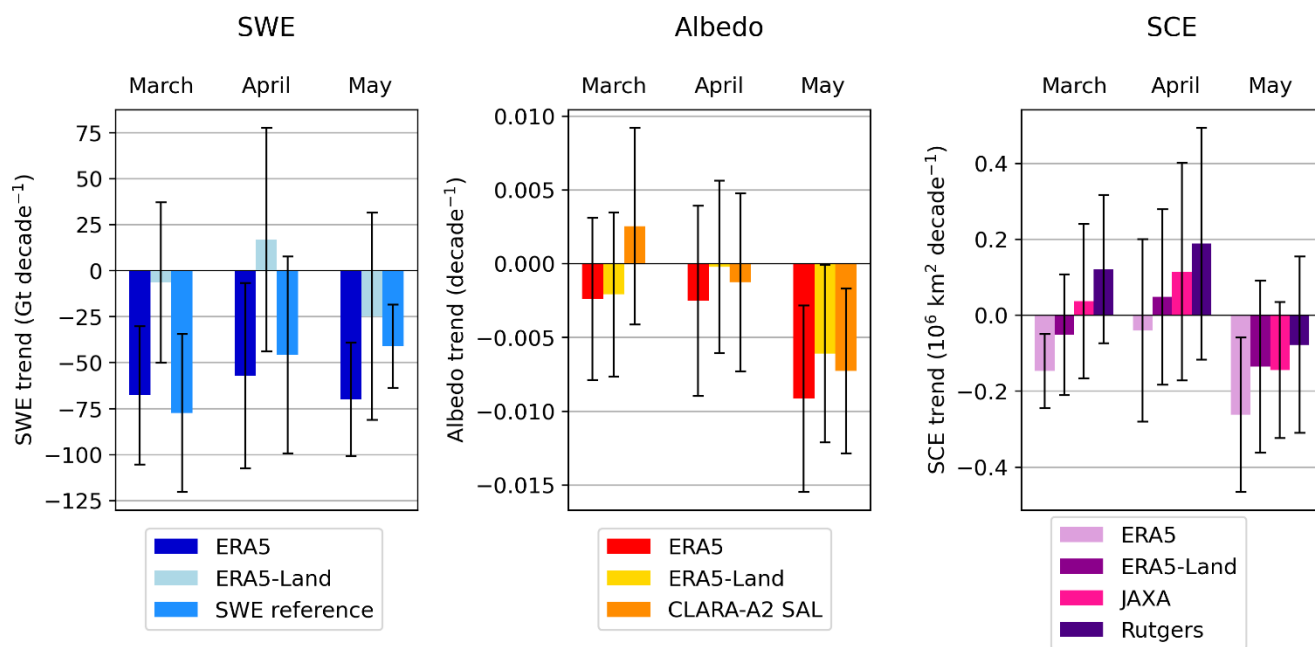
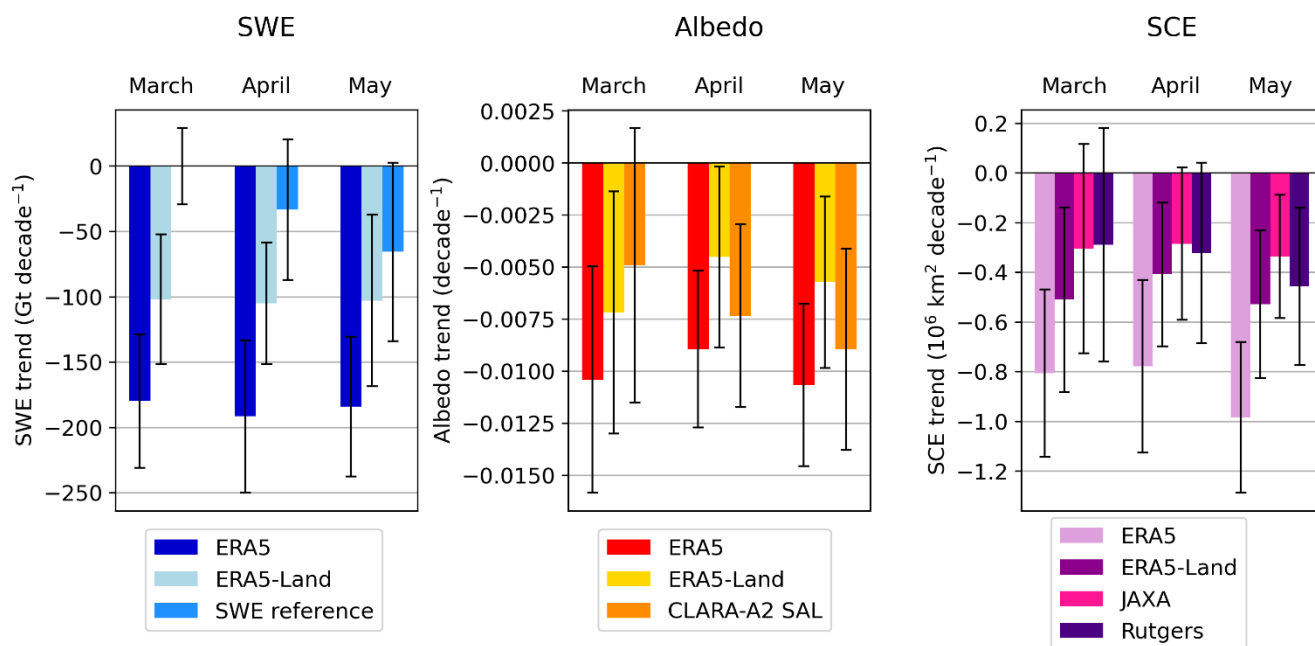**Figure 6. Trends in North America in 1982-2018. The error bars represent the 95% confidence intervals.**

370

Figure 7. Trends in Eurasia in 1982-2018. The error bars represent the 95% confidence intervals.

3.3 Spatial trends in SWE and albedo

375   The trends in SWE for the period 1982-2018 show large spatial variability between the datasets (Fig. 8, top row). The trends in April and May are shown in the Supplementary material (Figs. S3-S4). ERA5 detects mostly negative trends in the whole study region in March. ERA5-Land, in turn, shows negative trends in the western side of Eurasia and very weak trends in North America and in eastern Eurasia. The SWE reference data detect negative trends in northern part of North America but shows large variability in trends in Eurasia. All datasets indicate a positive trend in Lapland. The trends in March in albedo

380   (Fig. 8, bottom row) are more consistent between the datasets. There is a large area in southwestern part of Eurasia with a clear negative trend related to loss of low-latitude seasonal snow cover in every dataset. A positive trend is visible in Canada; however, the size of the area shows some variability between the datasets. Also, CLARA-A2 SAL detects a positive trend in southeastern Eurasia, which is not visible in ERA5 or ERA5-Land.

385   We additionally studied the trends for the period 2000-2018, as MODIS data are only available from year 2000 onwards. The SWE trends for the period 2000-2018 (Fig. 9, top row) are clearly more consistent with each other, which is most likely due to adding the IMS information to ERA5, which improves SWE estimates after 2004. The trends in April and May are shown in the Supplementary material (Figs. S5-S6). Overall, the trends are more prominent in 2000-2018 than in 1982-2018. All datasets detect negative trends in northeastern Canada, west coast of North America and western Eurasia in March.

390   Positive trends, in turn, are shown over a large area in Canada, Scandinavia and in many areas in Siberia. The positive trend in Canada is consistent with other studies and it is associated with cooling in spring season (Mudryk et al., 2018). The positive trend is very strong in Scandinavia, and it is detected by all the datasets. We additionally analyzed in situ snow depth measurement across Lapland (Fig. S7) to investigate, weather the positive trend is also visible in in situ measurements. For the period 1982-2018, the trend based on in situ measurements is negligible, but for 2000-2018, there is a statistically

395   significant positive trend (9.3 cm decade^{-1} in March), which is consistent with Figs. 8 and 9.

MODIS and CLARA-A2 SAL are consistent with each other, whereas ERA5 and ERA5-Land show some discrepancies in albedo trends. All datasets show a strong positive trend in albedo in Central Asia (fig. 9, bottom row), which is associated with an increase in snow cover over that area (Li et al., 2018). The albedo over Central Asia has been observed to increase

400   also in summer due to forestation (Li et al., 2018). Albedo has been increasing also over Canada, which is consistent with the positive SWE trend. Also, a negative trend is detected over Europe and western parts of Russia, where SWE has also been decreasing. Both ERA5 and ERA5-Land show a strong positive trend in northern Siberia, which is not as prominent in MODIS or CLARA-A2 SAL products. Also, MODIS and CLARA-A2 SAL show a negative trend in Central Siberia, which is not visible in ERA5 or ERA5-Land.
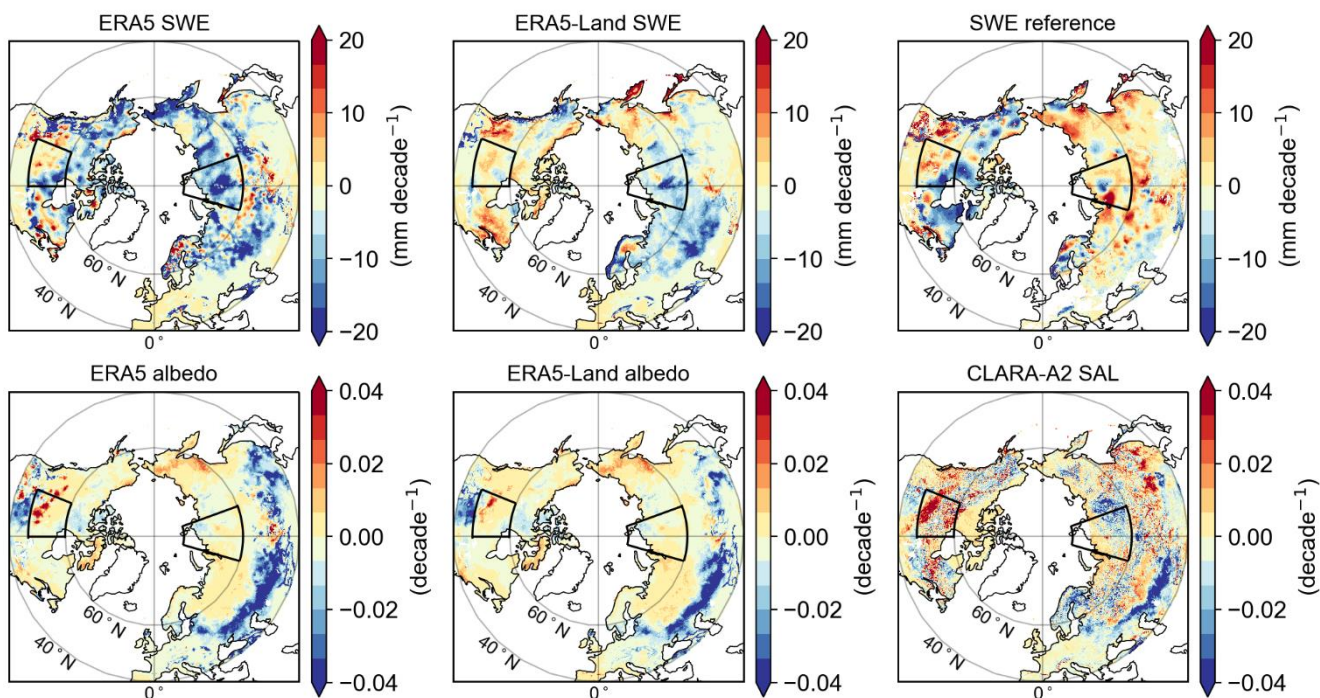
Figure 8. (top row) SWE trends in March 1982-2018. (bottom row) Albedo trends in March 1982-2018.
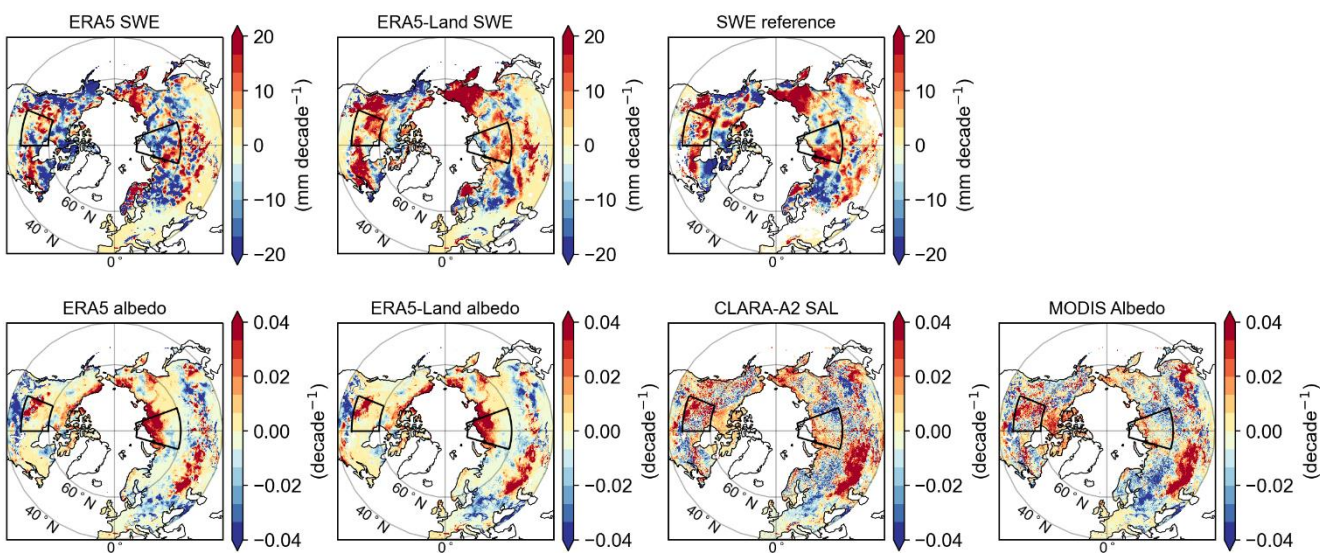

**Figure 9. (top row) SWE trends in March 2000-2018. (bottom row) Albedo trends in March 2000-2018.**

3.3 Regional trends

We additionally studied timeseries in smaller areas in the Western Siberia and the Canadian Prairies (areas marked in Figs 8 and 9). We chose these areas, because the trends in 1982-2018 show large differences between datasets but are more consistent in 2000-2018. In Siberia, both ERA5 and ERA5-Land overestimate SWE in the beginning of the study period (Fig 10, first and second row). The difference in SWE sum decreases throughout the study period and there is a clear drop in the difference between ERA5 and the SWE reference data in year 2004. After 2004, the difference is close to zero, with some annual variability. ERA5-Land does not show a clear improvement in 2004, but the difference is more stable throughout the study period.
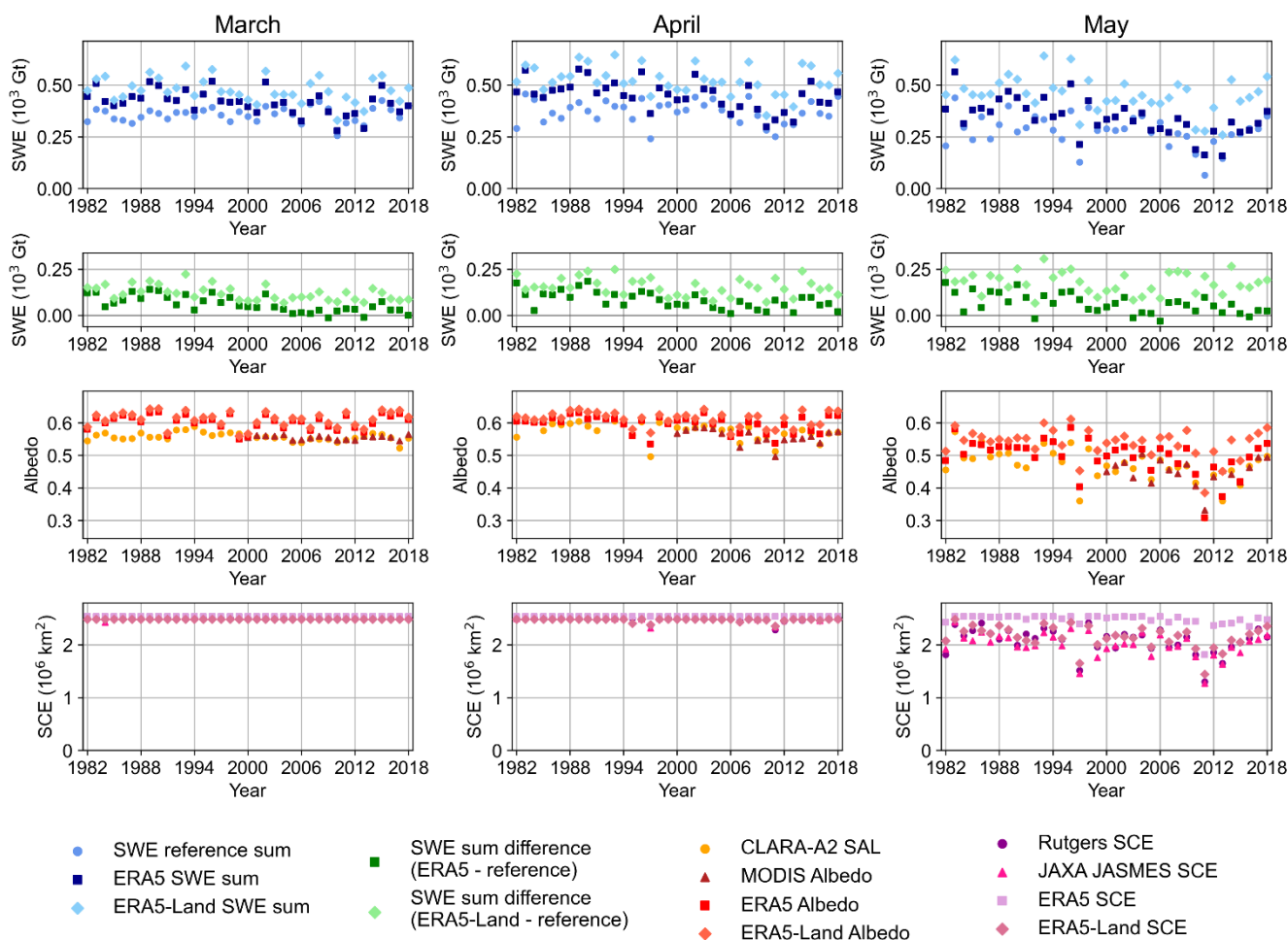
Figure 10. Timeseries in Western Siberia in (left) March, (middle) April and (right) May for SWE sum (top row), difference in SWE sum (second row), albedo (third row) and SCE (bottom row).The area is marked in Figs. 8 and 9.
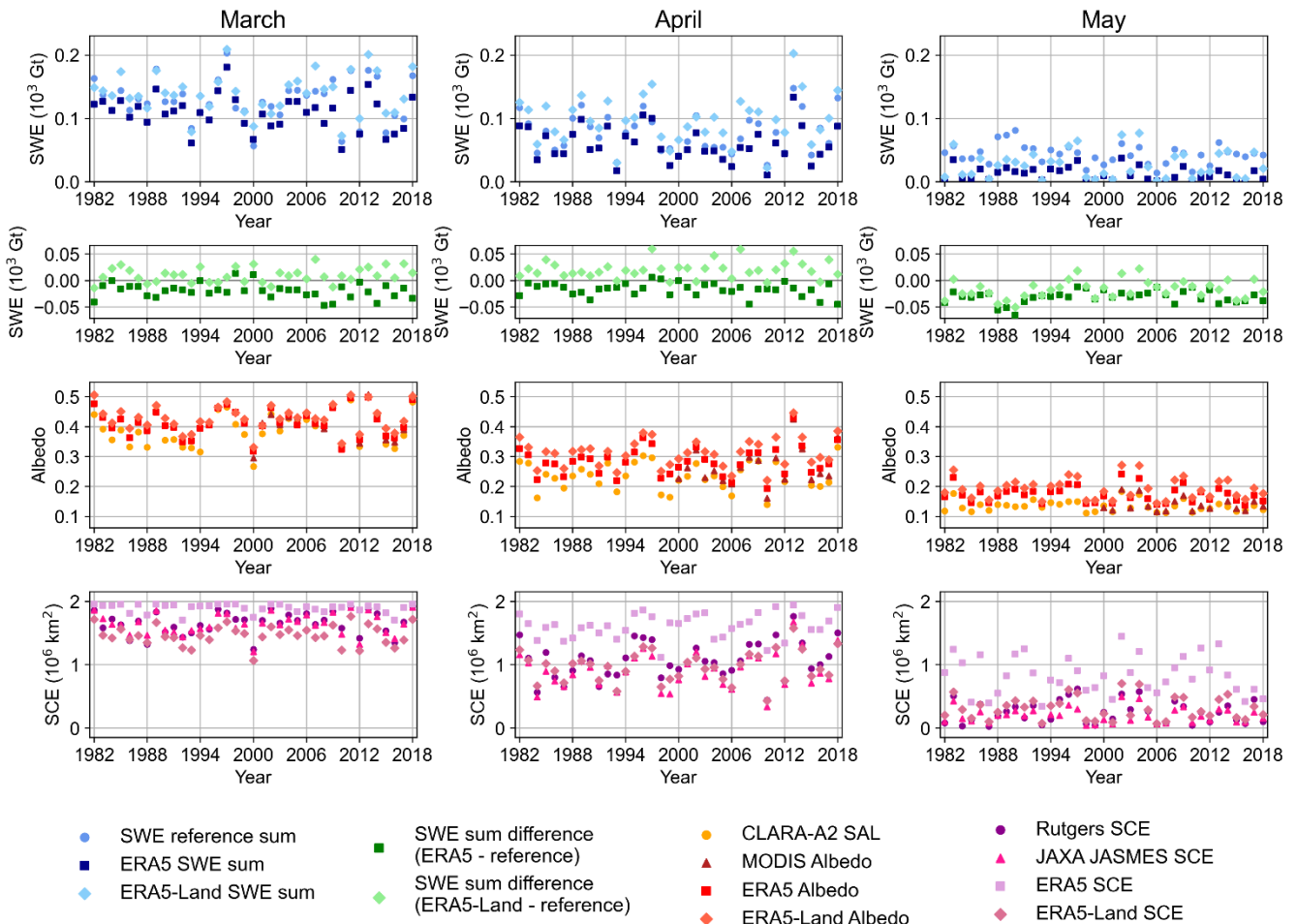
Figure 11. Timeseries in Canadian Prairies in (left) March, (middle) April and (right) May for SWE sum (top row), difference in SWE sum (second row), albedo (third row) and SCE (bottom row). The area is marked in Figs. 8 and 9.

Both ERA5 and ERA5-Land show a small overestimation in albedo (Fig 10, third row). The overestimation compared to satellite-based data is at its lowest in April. Even though there is a difference in the albedo values between ERA5, ERA5-Land and the satellite-based datasets, both ERA5 and ERA5-Land capture the annual variability quite accurately. All SCE datasets (Fig 10, bottom row) show that the whole area is covered with snow in March and April, with a few minor exceptions. In May, when the spring advances and melt season starts, the variability increases. ERA5 shows overestimation is SCE compared to other datasets, while ERA5-Land is very well in line with JAXA JASMES and Rutgers.

435   In the Canadian Prairies, the SWE estimates are quite consistent with each other (Fig. 11, first and second row). There is only a minor variability between the datasets and the difference varies from negative to positive. Especially in May, both ERA5 and ERA5-Land show mostly smaller SWE estimates than the SWE reference data. Contrary to Western Siberia, there is no clear drop in SWE sum difference in year 2004.

440   All the albedo datasets are very consistent in the Canadian Prairies in March, but when spring advances, the difference increases (Fig. 11, third row); in May, both ERA5 and ERA5-Land show a slight overestimation in albedo. Also, in SCE (Fig. 11, bottom row), the variability between the datasets increases when spring advances. ERA5 overestimates SCE also in this area throughout the spring season, and the overestimation is greatest in May. ERA5-Land, in turn, shows smaller SCE values in March compared to Rutgers and JAXA JASMES. In April and May, ERA5-Land, Rutgers and JAXA JASMES are
445   mostly consistent with each other. Both Figs. 10 and 11 illustrate that even though there are discrepancies between ERA5, ERA5-Land and the satellite-based datasets, both ERA5 and ERA5-Land are able to capture the interannual variability quite accurately.

4 Discussion

ERA5 and ERA5-Land show overall too large SWE sum estimates, which are mostly concentrated in the mountainous
450   regions (Figs. 1 and 2). The SWE estimates in the non-mountainous regions are better in line with the SWE reference data (Fig. S2). This result is consistent with other studies, as snow depth above 1500 m has been found to be unrealistically large in ERA5 (Hersbach et al., 2020). ERA5 has also shown a delayed ablation of deep snowpack in spring in Tibetan Plateau (Lei et al., 2022). The snowpack is presented in IFS with a single layer of snow which does not produce enough melting, and this results in excessively high snow depths (Hersbach et al., 2020).

455

Also, studies have shown that ERA5-Land overestimates snow depths more than ERA5 over the mountains (Monteiro and Morin, 2023; Muñoz-Sabater et al., 2021), which is consistent with our study. Both ERA5 and ERA5-Land show too high values in mountainous regions, but ERA5 has been found to perform better at the highest mountains (>3300 m), whereas ERA5-Land show improvements on mid-altitude mountains due to the higher resolution (Muñoz-Sabater et al., 2021). This
460   also mostly likely explains, why ERA5-Land overestimates SWE more than ERA5 (Fig. 2). The comparison between North America and Eurasia (Figs. 4 and 5) showed that ERA5 and ERA5-Land overestimate SWE more in North America, which likely results from the very high SWE values in Rocky Mountains. As the highest elevations of the Rocky Mountains exceed 3300 m, ERA5-Land shows even larger overestimation in SWE compared to ERA5.

465   The regional analysis (Sect. 3.3) showed that there is a large regional variability between the datasets. Even though ERA5 and ERA5-Land show overall larger SWE estimates, the difference is mostly opposite in Canadian Prairies. ERA5 shows

smaller SWE estimates throughout spring season, whereas for ERA5-Land, the difference decreases and drops under zero when spring advances (Fig. 11). However, also in these smaller regions, the difference between ERA5 and ERA5-Land stays the same, as ERA5-Land show larger SWE estimates than ERA5.

470

The SCE timeseries between ERA5-Land and the satellite-based datasets show only minor differences, while ERA5 notably overestimates SCE. That is, ERA5 tends to overestimate SCE, while ERA5-Land tends to overestimate SWE. The overestimation of SCE in ERA5 occurs in regions with shallow snowpack, which means that it does not convert to excessively large SWE values. ERA5-Land, in turn, overestimates SWE especially over mountainous regions with deep

475 snowpack. These areas are typically completely covered with snow and, therefore, overestimating SWE does not cause excessively high SCE values.

Timeseries of albedo are overall quite consistent between the datasets. Both ERA5 and ERA5-Land show a slight overestimation in albedo (Fig. 2) and when spring advances the difference slightly increases. Also, the analysis shows that

480 ERA5-Land shows moderately higher albedo values than ERA5. The discrepancy between satellite-based datasets and the reanalysis can be due to the different albedos used in the analysis. The satellite-based datasets provide estimates for black-sky albedo, whereas ERA5 and ERA5-Land provide estimates for blue-sky albedo. The black-sky albedo only accounts for the direct solar radiation, while the blue-sky albedo is for both direct and diffuse solar radiation (Schaepman-Strub et al., 2006). Typically, blue-sky albedo shows higher values than black-sky albedo (Manninen et al., 2012), which may cause

485 discrepancies in the comparison.

The comparison between the different albedo estimates in ERA5 and ERA5-Land (Fig. S1) showed only a slight difference between the albedo estimates and indicates that the differences between albedo estimates are smaller than typically. Typically, the albedo over snow and ice is 4-6% (absolute) higher under cloud cover than clear skies (Key et al., 2001). Fig.

490 10 shows that in March, the study area in Western Siberia is fully covered with snow. Therefore, we additionally compared the ERA5 and ERA5-Land albedo estimates over that area. The difference between white-sky albedo and blue-sky albedo for clear-sky only showed 1.1% (absolute) higher values (ranging from 0.4% to 1.7%), which is notably smaller difference than typically. Studies have shown that radiation quantities are slightly biased in ERA5 (Babar et al., 2019; Urraca et al., 2018), which would also affect albedo.

495

Even though there are discrepancies between ERA5 and ERA5-Land and the satellite-based datasets, both ERA5 and ERA5-Land are mostly able to capture the annual variability quite accurately. This finding is also consistent with other studies (Orsolini et al., 2019). Especially the regional analyses (Figs. 10 and 11) show large annual variability, which both ERA5 and ERA5-Land are mostly able to capture. For example, in Western Siberia (Fig. 10), there is a clear increase in all the

500   variables in May after year 2011, which all the datasets detect similarly. In Canadian Prairies (Fig. 11) albedo shows large interannual variability in March throughout the study period, which both ERA5 and ERA5-Land capture quite accurately.

The trends in 1982-2018 show considerable variability among the datasets (Fig. 3). ERA5 shows overall most prominent trends in all variables. Especially the trend in SWE differs considerably from ERA5-Land and the SWE reference data.
505   Recent studies have shown that there is a discontinuity in snow cover estimates in 2004, which is caused by adding the IMS information to ERA5 (Mortimer et al., 2020; Urraca and Gobron, 2021). This improves the SWE estimates after year 2004, but it decreases the stability of the timeseries, and, therefore, makes the trends less reliable. ERA5-Land does not exhibit the same discontinuity, which improves the stability of trends, but in turn, decreases the accuracy of snow cover estimates at the end of the study period. The satellite-based datasets can also exhibit discontinuities due to using different satellite
510   instruments, but typically these are taken into account so that the datasets are suitable for climate studies (Hori et al., 2017; Luojus et al., 2021).

IMS information is assimilated only on altitudes under 1500 m, so it does not improve snow cover estimates in mountainous regions. This most likely explains, why the discontinuity is more visible in Eurasia than in North America (Figs. 4 and 5). As
515   the Rocky Mountains account for a large fraction of SWE sum in North America, adding IMS has smaller effect on SWE sum estimate at continental scale. This phenomenon is also seen in the trends in North America and Eurasia (Figs. 6 and 7). The SWE trends in North America are similar in ERA5 and the SWE reference data (Fig. 6), while there is a large difference in Eurasia (Fig. 7). Since there is not a clear discontinuity visible in North America, it improves the stability of the trends and makes them more reliable. The downside is that the SWE values itself are not improved towards the end of the study
520   period. In Eurasia, in turn, the trends show a considerate difference between ERA5 and the SWE reference data, which cannot be even explained with the uncertainties. This suggests that the trends in 1982-2018 are not reliable, but the SWE estimates notably improve after year 2004 and are very similar with the SWE reference data. This conclusion is consistent with previous studies (Mortimer et al., 2020; Urraca and Gobron, 2021).

525   There are also uncertainties relates to the satellite-based datasets, which can affect the comparison. The satellite-based SWE is more reliable than before, but, still, some uncertainties do exist. The comparison between JAXA JASMES and in situ observations showed a slight overestimation in JAXA JASMES (Hori et al., 2017). Also, the difference between JAXA JASMES and Rutgers increases towards May, indicating that melting snow may pose a challenge to satellite-based snow detection. The uncertainty related to MCD43D51 product is overall very low, as we have only included the pixels with good
530   quality in the analysis. Also, CLARA-A2 SAL performs overall accurately over snow and ice (Anttila et al., 2016b), which increases the reliability of this analysis.

In mountainous regions, the high topographic variability can cause uncertainties in the satellite-based estimates, as the relatively coarse resolution of satellite-data is not ideal for mountainous regions. The complex terrain causes uncertainties in SWE estimates but averaging over multiple products can improve the accuracy (Mortimer et al., 2020). Mountains can also complicate albedo retrieval due to shadowing, but this is taken into account by making the topography correction for the CLARA-A2 SAL product (Anttila et al., 2016). Also, as mountains only represent a small fraction of the whole study area, they have limited effect on the overall albedo and SCE values.

5 Conclusions

We have evaluated snow cover properties in ERA5 and ERA5-Land and compared the timeseries and trends with several satellite-based datasets. Our study included SWE, SCE and albedo, which are the most important variables related to snow cover. Our study covers land areas north of 40 °N and the spring season from March to May in 1982-2018. The main findings in our study are as follows:

- Both ERA5 and ERA5-Land overestimate SWE, with ERA5-Land SWE estimates being the largest. The difference between ERA5-Land and SWE reference data remains at about 3000 Gt throughout the study period, which means that the NH total seasonal snow mass estimated by ERA5-Land is about two times higher in March and almost three times higher in May compared to the SWE reference data. The excessively high SWE is mostly due to the very large values over mountainous regions.

- There is a discontinuity in ERA5 around year 2004, since adding IMS from year 2004 onwards considerably improves SWE estimates but affects the temporal stability. ERA5-Land does not exhibit the same discontinuity, which improves the temporal stability of the trends, but in turn, decreases the accuracy of snow cover estimates at the end of the study period.

- Due to the discontinuity, ERA5 shows two or even three times larger decreasing trend than ERA5-Land and the SWE reference data: SWE trends in ERA5 range from -249 Gt decade^{-1} to -236 Gt decade^{-1} in spring, while the trends in ERA5-Land and the SWE reference data range from -124 Gt decade^{-1} to -77 Gt decade^{-1} in spring.

- ERA5 and ERA5-Land albedo estimates are quite consistent with the satellite-based datasets with only a slight overestimation. However, this discrepancy may be explained with the discrepancy between the used variables: the satellite-based datasets provide estimates for black-sky albedo, whereas ERA5 and ERA5-Land provide estimates for blue-sky albedo. Typically, the blue-sky albedo is slightly higher than the black-sky albedo, which may explain the difference. The negative trend in albedo is strongest in May, when it varies from -0.011 decade^{-1} to -0.006 decade^{-1} depending on the dataset.

- SCE is very accurately described in ERA5-Land, whereas ERA5 shows considerably larger values compared to the satellite-based datasets. Similar to albedo, the negative trends become more prominent when spring advances, and

565   in May, all the datasets show statistically significant negative trends. However, the negative trend detected by ERA5 (-1.22 million km^2 decade^{-1}) is about twice as large as the trends detected by other datasets (ranging from -0.66 million km^2 decade^{-1} to -0.50 million km^2 decade^{-1}).

- Despite the discrepancies in ERA5 and ERA5-Land with the satellite-based datasets, both are able to capture the interannual variability quite accurately.

Data availability

570 The bias-corrected SnowCCI data are available online at https://doi.org/10.1594/PANGAEA.911944. The Brown and Crocus v7 datasets are available from the original authors (please see Table 1 for references). MERRA-2 SWE data are available online at https://doi.org/10.5067/RKPHT8KC1Y1T. CLARA-A2 SAL data are available online at https://doi.org/10.5676/EUM_SAF_CM/CLARA_AVHRR/V002. MCD43D51 data are available online at 575 https://ladsweb.modaps.eosdis.nasa.gov/archive/allData/6/MCD43D51/. Rutgers SCE data are available online at https://nsidc.org/data/g10035/versions/1. JAXA JASMES SCE data are available online at https://www.eorc.jaxa.jp/JASMES/index.html. ERA5 and ERA5-Land are available online at https://cds.climate.copernicus.eu.

Author Contributions

580 KK conducted the analysis and drafted the manuscript. All authors contributed to manuscript review and editing.

Competing interests

The authors declare that they have no conflict of interest.

Acknowledgements

References

Ångström, A.: The albedo of various surfaces of ground. Geografiska Annaler, 7(4), 323-342, https://doi.org/10.1080/20014422.1925.11881121, 1925.

590   Anttila, K., Jääskeläinen, E., Riihelä, A., Manninen, T., Andersson, K., and Hollman, R.: Algorithm theoretical basis document: CM SAF cloud, albedo, radiation data record Ed. 2—Surface Albedo, https://doi.org/10.5676/EUM_SAF_CM/CLARA_AVHRR/V002, 2016.

Anttila, K., Manninen, T., Jääskeläinen, E., Riihelä, A., Hollman, R.: Validation report: CM SAF cloud, albedo, radiation
595   data record Ed. 2—Surface Albedo, https://doi.org/10.5676/EUM_SAF_CM/CLARA_AVHRR/V002, 2016b

Babar, B., Graversen, R., and Boström, T.: Solar radiation estimation at high latitudes: Assessment of the CMSAF databases, ASR and ERA5, Sol. Energy, 182, 397-411, https://doi.org/10.1016/j.solener.2019.02.058, 2019.

600   Barnett, T., Adam, J. and Lettenmaier, D.: Potential impacts of a warming climate on water availability in snow-dominated regions, Nature, 438, 303–309, https://doi.org/10.1038/nature04141, 2005.

Bian, Q., Xu, Z., Zhao, L., Zhang, Y. F., Zheng, H., Shi, C., Zhang, S., Xie, C. and Yang, Z. L.: Evaluation and intercomparison of multiple snow water equivalent products over the Tibetan Plateau, J. Hydrometeorol., 20(10), 2043-
605   2055., https://doi.org/10.1175/JHM-D-19-0011.1, 2019.

Bormann, K. J., Brown, R. D., Derksen, C., and Painter, T. H.: Estimating snow-cover trends from space, Nat. Clim. Change, 8, 924–928. https://doi.org/10.1038/s41558-018-0318-3, 2018.

610   Brown, R. D., Brasnett, B., and Robinson, D.: Gridded North American monthly snow depth and snow water equivalent for GCM evaluation, Atmos.-Ocean, 41, 1–14, https://doi.org/10.3137/ao.410101, 2003.

Brown, R., Derksen, C., and Wang, L.: A multi-data set analysis of variability and change in Arctic spring snow cover extent, 1967–2008, J. Geophys Res.-Atmos., 115(D16)., https://doi.org/10.1029/2010JD013975, 2010.
615
Brun, E., Vionnet, V., Boone, A., Decharme, B., Peings, Y., Vallette, R., Karbou, F., and Morin, S.: Simulation of northern Eurasian local snow depth, mass, and density using a detailed snowpack model and meteorological reanalyses, J. Hydrometeorol., 14, 203–219, https://doi.org/10.1175/JHM-D-12-012.1, 2013.

620   Callaghan, T. V., Johansson, M., Brown, R. D., Groisman, P. Y., Labba, N., Radionov, V., Bradley, R. S., Blangy, S., Bulygina, O. N., Christensen, T. R., Colman, J. E., Essery, R. L. H., Forbes,B. C., Forchhammer, M. C., Golubev, V. N., Honrath, R. E., Ju-day, G. P., Meshcherskaya, A. V., Phoenix, G. K., Pomeroy, J., Rautio, A., Robinson, D. A., Schmidt, N.

M., Serreze, M. C.,Shevchenko, V. P., Shiklomanov, A. I., Shmakin, A. B., Sköld, P., Sturm, M., Woo, M.-K., and Wood, E. F.: Multiple effects of changes in arctic snow cover, Ambio, 40, 32–45, https://doi.org/10.1007/s13280-011-0213-x, 2011.

625

Derksen, C. and Brown, R.: Spring snow cover extent reductions in the 2008–2012 period exceeding climate model projections, Geophys. Res. Lett., 39, L19504, https://doi.org/10.1029/2012GL053387, 2012.

Derksen, C., and Mudryk, L.: Assessment of Arctic Seasonal Snow Cover Rates of Change, Cryosphere Discussions, 1-21., 630 https://doi.org/10.5194/tc-2022-197, 2022.

Déry, S. J., and Brown, R. D.: Recent Northern Hemisphere snow cover extent trends and implications for the snow albedo feedback, Geophys. Res. Lett., 34, L22504, https://doi.org/10.1029/2007GL031474, 2007.

635 Douville, H., Chauvin, F., Planton, S., Royer, J. F., Salas-Melia, D., and Tyteca, S.: Sensitivity of the hydrological cycle to increasing amounts of greenhouse gases and aerosols, Clim. Dynam., 20, 45–68. https://doi.org/10.1007/s00382-002-0259-3, 2002.

Estilow, T. W., Young, A. H., and Robinson, D. A.: A long-term Northern Hemisphere snow cover extent data record for 640 climate studies and monitoring, Earth Syst. Sci. Data, 7(1), 137-142., https://doi.org/10.5194/essd-7-137-2015, 2015.

Fierz, C., Armstrong, R. L., Durand, Y., Etchevers, P., Greene, E., McClung, D. M., Nishimura, K., Satyawali, P.K. and Sokratov, S.A.: The International Classification for Seasonal Snow on the Ground, IHP-VII Technical Documents in Hydrology No. 83, IACS Contribution No. 1, UNESCO-IHP, 2009.

645

Flanner, M. G., Shell, K. M., Barlage, M., Perovich, D. K., and Tschudi, M. A.: Radiative forcing and albedo feedback from the Northern Hemisphere cryosphere between 1979 and 2008, Nat. Geosci., 4, 151-155, https://doi.org/10.1038/ngeo1062, 2011.

650 Gelaro, R., McCarty, W., Suárez, M. J., Todling, R., Molod, A., Takacs, L., Randles, C. A., Darmenov, A., Bosilovich, M. G., Reichle, R., Wargan, K., Coy, L., Cullather, R., Draper, C., Akella, S., Buchard, V., Conaty, A., da Silva, A. M., Gu, W., Kim, G.-K., Koster, R., Lucchesi, R., Merkova, D., Nielsen, J. E., Partyka, G., Pawson, S., Putman, W., Rienecker, M., Schubert, S. D., Sienkiewicz, M., and Zhao, B.: The modern-era retrospective analysis for research and applications, version 2 (MERRA-2), J. Climate, 30, 5419-5454, https://doi.org/10.1175/JCLI-D-16-0758.1, 2017.

655

Global Modeling and Assimilation Office (GMAO): MERRA-2 tavg1_2d_lnd_Nx: 2d, 1-Hourly, Time-Averaged, Single-Level, Assimilation, Land Surface Diagnostics V5.12.4 (M2T1NXLND), Goddard Earth Sciences Data and Information Services Center (GES DISC) [data set], https://doi.org/10.5067/RKPHT8KC1Y1T, 2015.

660 Guo H. and Yang Y.: Spring snow-albedo feedback from satellite observation, reanalysis and model simulations over the Northern Hemisphere, Sci. China Earth Sci., 65(8): 1463–1476, https://doi.org/10.1007/s11430-021-9913-1, 2022.

Hall, N. D., Stuntz, B. B., and Abrams, R. H.: Climate change and freshwater resources, Natural Resources & Environment, 22, 30-35, 2008.

665

Hernández-Henríquez, M. A., Déry, S. J., and Derksen, C.: Polar amplification and elevation-dependence in trends of Northern Hemisphere snow cover extent, 1971–2014, Environ. Res. Lett., 10, 044010. https://doi.org/10.1088/1748-9326/10/4/044010, 2015.

670 Hersbach, H., Bell, B., Berrisford, P., Hirahara, S., Horányi, A., Muñoz-Sabater, J., Nicolas, J., Peubey, C., Radu, R., Schepers, D., Simmons, A., Soci, C., Abdalla, S., Abellan, X., Balsamo, G., Bechtold, P., Biavati, P., Bidlot, J., Bonavita, M., De Chiara, G., Dahlgren, P., Dee, D., Diamantakis, M., Dragani, R., Flemming, J., Forbes, R., Fuentes, M., Geer, A., Haimberger, H., Healy, S., Hogan, R. J., Hólm, E., Janisková, M., Keeley, S., Laloyaux, P., Lopez, P., Lupu, C., Radnoti, G., de Rosnay, P., Rozum, I., Vamborg, F., Villaume, S., and Thépaut, J.-N.: The ERA5 global reanalysis, Q. J. Roy.
675 Meteor. Soc., 146(730), 1999-2049, https://doi.org/10.1002/qj.3803, 2020.

Hori, M., Sugiura, K., Kobayashi, K., Aoki, T., Tanikawa, T., Kuchiki, K., Niwano, M., and Enomoto, H.: A 38-year (1978–2015) Northern Hemisphere daily snow cover extent product derived using consistent objective criteria from satellite-borne optical sensors, Remote Sens. Environ., 191, 402-418, https://doi.org/10.1016/j.rse.2017.01.023, 2017.

680

Jia, A., Wang, D., Liang, S., Peng, J., and Yu, Y.: Global Daily Actual and Snow-Free Blue-Sky Land Surface Albedo Climatology From 20-Year MODIS Products, J. Geophys Res.-Atmos., 127(8), e2021JD035987, https://doi.org/10.1029/2021JD035987, 2022.

685 Karlsson, Karl-Göran; Anttila, Kati; Trentmann, Jörg; Stengel, Martin; Meirink, Jan Fokke; Devasthale, Abhay; Hanschmann, Timo; Kothe, Steffen; Jääskeläinen, Emmihenna; Sedlar, Joseph; Benas, Nikos; van Zadelhoff, Gerd-Jan; Schlundt, Cornelia; Stein, Diana; Finkensieper, Stephan; Håkansson, Nina; Hollmann, Rainer; Fuchs, Petra; Werscheck, Martin: CLARA-A2: CM SAF cLoud, Albedo and surface RAdiation dataset from AVHRR data - Edition 2, Satellite Application Facility on Climate Monitoring, https://doi.org/10.5676/EUM_SAF_CM/CLARA_AVHRR/V002, 2017.

690

Key, J. R., Wang, X., Stoeve, J. C., and Fowler, C.: Estimating the cloudy-sky albedo of sea ice and snow from space, J. Geophys Res.-Atmos., 106(D12), 12489-12497, https://doi.org/10.1029/2001JD900069, 2001.

Kundzewicz, Z. W., Mata, L. J., Arnell, N. W., Döll, P., Jimenez, B., Miller, K., Oki, T., Şen, Z, and Shiklomanov, I.: The

695   implications of projected climate change for freshwater resources and their management, Hydrolog. Sci. J., 53, 3-10 https://doi.org/10.1623/hysj.53.1.3, 2008.

Lei, Y., Pan, J., Xiong, C., Jiang, L., and Shi, J.: Snow depth and snow cover over the Tibetan Plateau observed from space in against ERA5: matters of scale, Clim. Dynam., 1-19, https://doi.org/10.1007/s00382-022-06376-0, 2022.

700

Li, D., M. L. Wrzesien, M. Durand, J. Adam, and D. P. Lettenmaier: How much runoff originates as snow in the western United States, and how will that change in the future?, Geophys. Res. Lett., 44, 6163–6172, https://doi.org/10.1002/2017GL073551, 2017.

705   Li, Q., Ma, M., Wu, X., and Yang, H.: Snow cover and vegetation-induced decrease in global albedo from 2002 to 2016. J. Geophys Res.-Atmos., 123(1), 124-138, https://doi.org/10.1002/2017JD027010, 2018.

Li, Q., Yang, T., and Li, L.: Evaluation of snow depth and snow cover represented by multiple datasets over the Tianshan Mountains: Remote sensing, reanalysis, and simulation, Int. J. Climatol., 42(8), 4223-4239, https://doi.org/10.1002/joc.7459,

710   2022.

Luojus, K., Pulliainen, J., Takala, M., Lemmetyinen, J., Moisander, M., Mortimer, C., Derksen, C., Hiltunen, M., Smolander, T., Ikonen, J., Cohen, J., Veijola, K., and Venäläinen, P.: GlobSnow v3.0 Northern Hemisphere snow water equivalent dataset, Sci. Data, https://doi.org/10.1038/s41597-021-00939-2, 2021.

715

Magnusson, J., Nævdal, G., Matt, F., Burkhart, J. F., and Winstral, A.: Improving hydropower inflow forecasts by assimilating snow data, Hydrol. Res., 51, 226-237, https://doi.org/10.2166/nh.2020.025, 2020.

Manninen, T., Riihelä, A., and de Leeuw, G.: Atmospheric effect on the ground-based measurements of broadband surface

720   albedo, Atmos. Meas. Tech., 5(11), 2675-2688, https://doi.org/10.5194/amt-5-2675-2012, 2012.

Manninen, T., Jääskeläinen, E., and Riihelä, A.: Black and white-sky albedo values of snow: In situ relationships for AVHRR-based estimation using CLARA-A2 SAL, Can. J. Remote Sens., 45(3-4), 350-367, https://doi.org/10.1080/07038992.2019.1632177, 2019.

725

Metsämäki, S., Böttcher, K., Pulliainen, J., Luojus, K., Cohen, J., Takala, M., Mattila, O.-P., Schwaizer, G., Derksen, C. and Koponen, S.: The accuracy of snow melt-off day derived from optical and microwave radiometer data—A study for Europe, Remote Sens. Environ., 211, 1-12. https://doi.org/10.1016/j.rse.2018.03.029, 2018.

730   Monteiro, D., and Morin, S.: Multi-decadal past winter temperature, precipitation and snow cover information over the European Alps using multiple datasets, EGUsphere, 1-62, https://doi.org/10.5194/egusphere-2023-166, 2023.

Mortimer, C., Mudryk, L., Derksen, C., Luojus, K., Brown, R., Kelly, R., and Tedesco, M.: Evaluation of long-term Northern Hemisphere snow water equivalent products, Cryosphere, 14, 1579-1594, https://doi.org/10.5194/tc-14-1579-2020,
735   2020.

Mortimer, C., Mudryk, L., Derksen, C., Brady, M., Luojus, K., Venäläinen, P., Moisander, M., Lemmetyinen, J., Takala, M., Tanis, C., and Pulliainen, J.: Benchmarking algorithm changes to the Snow CCI+ snow water equivalent product, Remote Sens. Environ., 274, 112988, https://doi.org/10.1016/j.rse.2022.112988, 2022.

740

Mudryk, L. R., Derksen, C., Howell, S., Laliberté, F., Thackeray, C., Sospedra-Alfonso, R., Vionnet, V., Kushner, P.J., and Brown, R.: Canadian snow and sea ice: historical trends and projections, Cryosphere, 12(4), 1157-1176, https://doi.org/10.5194/tc-12-1157-2018, 2018.

745   Mudryk, L., Santolaria-Otín, M., Krinner, G., Ménégoz, M., Derksen, C., Brutel-Vuilmet, C., Brady, M., and Essery, R.: Historical Northern Hemisphere snow cover trends and projected changes in the CMIP6 multi-model ensemble, Cryosphere, 14, 2495-2514, https://doi.org/10.5194/tc-14-2495-2020, 2020.

Muñoz-Sabater, J., Dutra, E., Agustí-Panareda, A., Albergel, C., Arduini, G., Balsamo, G., Boussetta, B., Choulga, M.,
750   Harrigan, S., Hersbach, H., Martens, B., Miralles, D. G., Piles, M., Rodríguez-Fernández, N. J., Zsoter, E., Buontempo, C., and Thépaut, J. N.: ERA5-Land: A state-of-the-art global reanalysis dataset for land applications, Earth Syst. Sci. Data, 13(9), 4349-4383, https://doi.org/10.5194/essd-13-4349-2021, 2021.

Musselman, K. N., Addor, N., Vano, J. A., and Molotch, N. P.: Winter melt trends portend widespread declines in snow
755   water resources, Nat. Clim. Change, 11(5), 418-424, https://doi.org/10.1038/s41558-021-01014-9, 2021.

Orsolini, Y., Wegmann, M., Dutra, E., Liu, B., Balsamo, G., Yang, K., de Rosnay, P., Zhu, C., Wang, W., Senan, R. and Arduini, G. Evaluation of snow depth and snow cover over the Tibetan Plateau in global reanalyses using in situ and satellite remote sensing observations, Cryosphere, 13(8), 2221-2239, https://doi.org/10.5194/tc-13-2221-2019, 2019.

760

Qu, X. and Hall, A.: Surface contribution to planetary albedo variability in cryosphere regions, J. Climate, 18, 5239–5252. https://doi.org/10.1175/JCLI3555.1, 2005.

Pulliainen, J., Luojus, K., Derksen, C., Mudryk, L., Lemmetyinen, J., Salminen, M., Ikonen, J., Takala, M., Cohen, J.,
765 Smolander, T., and Norberg, J.: Patterns and trends of Northern Hemisphere snow mass from 1980 to 2018, Nature, 581, 294-298, https://doi.org/10.1038/s41586-020-2258-0, 2020.

Pohl, C., Istomina, L., Tietsche, S., Jäkel, E., Stapf, J., Spreen, G., and Heygster, G.: Broadband albedo of Arctic sea ice from MERIS optical data, Cryosphere, 14(1), 165-182, https://doi.org/10.5194/tc-14-165-2020, 2020.

770

Riihelä, A., Manninen, T., Laine, V., Andersson, K., and Kaspar, F.: CLARA-SAL: a global 28 yr timeseries of Earth's black-sky surface albedo, Atmos. Chem. Phys., 13(7), 3743-3762, https://doi.org/10.5194/acp-13-3743-2013, 2013

Robinson, D. A., and T. W. Estilow.: Rutgers Northern Hemisphere 24 km Weekly Snow Cover Extent, September 1980
775 Onward, Version 1 [Data Set]. Boulder, Colorado USA. National Snow and Ice Data Center. https://doi.org/10.7265/zzbm-2w05. Date Accessed 02-28-2022, 2021.

Räisänen, J.: Warmer climate: less or more snow?, Clim. Dyn., 30, 307-319 https://doi.org/10.1007/s00382-007-0289-y, 2008.

780

Räisänen, J.: Changes in March mean snow water equivalent since the mid-twentieth century and the contributing factors in reanalyses and CMIP6 climate models, Cryosphere Discussions, https://doi.org/10.5194/tc-2022-248, 1-29, 2023.

Schaaf, C., and Wang, Z.: MODIS/Terra+Aqua BRDF/Albedo Black Sky Albedo Shortwave Daily L3 Global 30ArcSec
785 CMG V061 [Data set]. NASA EOSDIS Land Processes DAAC. Accessed 2022-06-01 from https://doi.org/10.5067/MODIS/MCD43D51.061, 2021a.

Schaaf, C., and Wang, Z.: MODIS/Terra+Aqua BRDF/Albedo QA BRDF Quality Daily L3 Global 30ArcSec CMG V061
[Data set]. NASA EOSDIS Land Processes DAAC. Accessed 2022-08-18 from
790   https://doi.org/10.5067/MODIS/MCD43D31.061, 2021b.

Schaepman-Strub, G., Schaepman, M. E., Painter, T. H., Dangel, S., and Martonchik, J. V.: Reflectance quantities in optical
remote sensing—Definitions and case studies, Remote Sens. Environ., 103(1), 27-42,
https://doi.org/10.1016/j.rse.2006.03.002, 2006.

795

Sen, P. K.: Estimates of the regression coefficient based on Kendall's tau, J. Am. Stat. Assoc., 63(324), 1379–1389.
https://doi.org/10.2307/2285891, 1968.

Shikwambana, L., and Sivakumar, V.: Global distribution of aerosol optical depth in 2015 using CALIPSO level 3 data, J.
800   Atmos. Sol.-Terr. Phys., 173, 150-159, https://doi.org/10.1016/j.jastp.2018.04.003, 2018.

Smith, R., Zagona, E., Kasprzyk, J., Bonham, N., Alexander, E., Butler, A., Praire, J., and Jerla, C.: Decision Science Can
Help Address the Challenges of Long-Term Planning in the Colorado River Basin, J. Am. Water Resour. As., 58(5), 735-
745., https://doi.org/10.1111/1752-1688.12985, 2022.

805

Takala, M., Pulliainen, J., Metsämäki, S. J., and Koskinen, J. T.: Detection of snowmelt using spaceborne microwave
radiometer data in Eurasia from 1979 to 2007, IEEE T. Geosci. Remote, 47(9), 2996-3007.
https://doi.org/10.1109/TGRS.2009.2018442, 2009.

810   Tedesco, M., Brodzik, M., Armstrong, R., Savoie, M., and Ramage, J.: Pan arctic terrestrial snowmelt trends (1979–2008)
from spaceborne passive microwave data and correlation with the Arctic Oscillation, Geophys. Res. Lett., 36(21), L21402.
https://doi.org/10.1029/2009GL039672, 2009.

Theil, H.: A rank-invariant method of linear and polynomial regression analysis (Parts 1–3), K. Ned. Akad. Van. Wet. A, 53,
815   386–392, 521–525, 1397–1412, 1950.

Trenberth, K. E. and Fasullo, J. T.: Global warming due to increasing absorbed solar radiation, Geophys. Res. Lett., 36,
L07706. https://doi.org/10.1029/2009GL03752, 2009.

820   Urraca, R., Huld, T., Gracia-Amillo, A., Martinez-de-Pison, F. J., Kaspar, F., and Sanz-Garcia, A.: Evaluation of global horizontal irradiance estimates from ERA5 and COSMO-REA6 reanalyses using ground and satellite-based data, Sol. Energy, 164, 339-354, https://doi.org/10.1016/j.solener.2018.02.059, 2018.

Urraca, R., and Gobron, N. Stability of long-term satellite and reanalysis products to monitor snow cover trends, Cryosphere

825   Discussions, 1-36, 2021.

Van Vliet, M. T. H., Van Beek, L. P. H., Eisner, S., Flörke, M., Wada, Y., and Bierkens, M. F. P.: Multi-model assessment of global hydropower and cooling water discharge potential under climate change, Glob. Environ. Change, 40, 156-170, https://doi.org/10.1016/j.gloenvcha.2016.07.007, 2016.

830

Xiaona, C., Shunlin, L., and Yaping, Y.: Differences in snow-induced radiative forcing estimated from satellite and reanalysis surface albedo datasets over the Northern Hemisphere landmass for the overlapping period of 1982–2012, Environ. Res. Commun., 2(9), 091001, https://doi.org/10.1088/2515-7620/abb3b8, 2020.